



Society of Petroleum Engineers

**SPE-177549-MS**

## **Efficient Use of Data Analytics in Optimization of Hydraulic Fracturing in Unconventional Reservoirs**

C. Temizel, Aera Energy; S. Purwar, A. Abdullayev, and K. Urrutia, Halliburton; Aditya Tiwari, Consultant, Sinem Setenay Erdogan, Turkish Petroleum Corp.

Copyright 2015, Society of Petroleum Engineers

This paper was prepared for presentation at the Abu Dhabi International Petroleum Exhibition and Conference held in Abu Dhabi, UAE, 9–12 November 2015.

This paper was selected for presentation by an SPE program committee following review of information contained in an abstract submitted by the author(s). Contents of the paper have not been reviewed by the Society of Petroleum Engineers and are subject to correction by the author(s). The material does not necessarily reflect any position of the Society of Petroleum Engineers, its officers, or members. Electronic reproduction, distribution, or storage of any part of this paper without the written consent of the Society of Petroleum Engineers is prohibited. Permission to reproduce in print is restricted to an abstract of not more than 300 words; illustrations may not be copied. The abstract must contain conspicuous acknowledgment of SPE copyright.

### **Abstract**

Hydraulic fracturing operations affect reservoir flow dynamics and increase production in unconventional tight reservoirs. The control of fracture growth and geometry presents challenges in formations in which the boundary lithologies are not highly stressed in comparison to the pay zone, thus failing to prevent the upward migration of fractures. Several factors influence the growth and geometry of fractures, including reservoir, wellbore, and fluid/proppant parameters. Successful results require a thorough knowledge of reservoir parameters, including stress distribution and the appropriate use of corresponding wellbore components and fluid/proppant. The success of a hydraulic fracturing treatment is highly correlated with control of the created fracture geometry.

This paper discusses a study in which a numerical fracture model is used to design the fractures in a tight oil reservoir. Fracture treatment designs include the selection of fracturing fluids, additives, proppant materials, injection rate, pumping schedule, and fracture dimensions. Using the fracture model, a statistically representative synthetic set of data is generated for each parameter to build data-driven models.

The performance of the data-driven models is validated by comparing the results to a numerical model, and considering the significance of parameters, including size, number, location, phasing angle of perforations, fluid and proppant type, rock strength, porosity, and permeability on the fracture design optimization using various fracture models. Data-driven predictive models are generated by using neural networks (NN) and support vector machine (SVM) algorithms. Optimum values of model parameters are also investigated.

The SVM and NN models are used to optimize the fracturing treatments per well, and are evaluated based on accuracy and computational complexity. Based on the performances of the models, model parameters are adjusted to obtain fit-for-purpose well-based hydraulic fracturing models.

### **Data-Driven Analytics**

Data about location and potential quantity has the potential to improve the fracturing process significantly and oil and gas companies can look forward to increasing their production levels as they gain new insight

into drilling locations from data received. If analyzed properly, the data can make the process less expensive and faster.

Mattar et al. (2006) provides a brief history of data analytics in the field of data-driven analytics for production data. Most of the work in analytics performed in the industry has been based on analytical models based on known mathematical theories. One of the first implementations of analytics was completed by Arps (1945). The authors correlated production data in the petroleum literature and are considered to be an essential starting point for analysis. Mattar and McNeil (1997) extended the work to provide an analysis/interpretation methodology for production data on a per-well basis. Li and Horne (2005) further provided a theoretical basis for some common production analysis relations. Blasingame and Rushing (2005) provided a synopsis of the historical methods used for simplified production analysis. Camacho and Raghavan (1989) provided the theoretical basis for boundary-dominated flow in solution gas-drive reservoirs. Fetkovich (1980) provided the analytical basis for production decline curves. These were extended to fractured wells by Agarwal et al. (1999) and Araya and Ozkan (2002) on the use of production decline type curve analysis for vertical, fractured, and horizontal wells. Fuentes-Cruz et al. (2004) provided extensions of the decline type curve analysis approach for a variety of cases in naturally fractured reservoirs.

While all of the discussed provide analytics primarily derived on known in reservoir physics, there is not much work completed purely on production diagnostics and key performance indicators (KPIs) based purely on data. One of the reasons could be that production data is normally not "high frequency" (or data available every few seconds or so), and hence traditional data mining techniques could not be applied. Anderson and Matter (2003) and Matter and Anderson (2004) provide guidelines and examples for the diagnosis of production data with regard to model-based analysis (type curves). Kabir and Izgec (2006) provide guidance on the diagnosis pressure-rate data with an emphasis on characterizing the reservoir production mechanism. Lastly, Bondar (2001) summarizes the modern and historical methods of analyzing water-oil-ratio (WOR) and water cut (fw) data from the perspective of characterizing the reservoir drive mechanism(s) and estimating reserves.

A more common approach used by the industry has mostly been to use proxy models or response surface methodology (RSM). RSM is used to model complex phenomena like production from oil and gas reservoirs by relating multiple explanatory variables to one or more response variables. RSM is useful for modeling, improving, and optimizing processes, and it has been widely applied in several areas, such as agriculture, industrial production engineering, and petroleum reservoir engineering. The initial development of RSM is generally attributed to Box and Wilson (1951). The great advantage of RSM is that it is easy to apply even when little is known about the phenomena being modeled.

There are various ways to implement RSM, but there are three typical components of RSM in applied analysis:

- The experimental design for defining the set of explanatory variables.
- A proxy model, which relates the response variable to the explanatory variables.
- An optimization method to estimate the marginal impacts of the explanatory variables on the response variable.

One of the criticisms of RSM is that it is too abstract and there is variability and the potential for bias in the estimation of the relationships and therefore in predicted values. However, more detailed modeling entails costs (in resources and time), and the value derived from additional effort cannot exceed the costs. RSM seeks to balance these costs and benefits, ideally on a case by case basis. The optimal design depends on the objective of the problem, the data available, and on the magnitude of the decision being made. In some cases, less detail and less iteration will be acceptable, while in other cases, the need for additional accuracy will justify more detailed specifications and more iteration. Several methods for RSM and experimental design have been proposed in the literature and the most popular methods are described in

the remainder of this chapter. Most methods have been devised to address specific scientific and engineering problems.

While the methods described are largely mathematically driven functions that substitute large numerical simulation cases by replicating simulation model output, they provide fast-approximated solutions to be used efficiently in the development planning, uncertainty analysis, and operational design optimization. The most frequently used proxy models in the oil and gas industry are reduced order models and response surfaces that reduces simulation run-time by approximating the problem and/or the solution space (Kalantari et al. 2012). Response surfaces are categorized as statistical-based proxy models that require a large number of simulation runs to facilitate optimization and uncertainty analysis. As stated by Mohaghegh (2014), there are two main problems associated with statistics, especially when applied to problems with well-defined physics behind them: a) the issue of "correlation vs. causality," and b) imposing a predefined functional form, such as linear, polynomial, exponential, etc., to the data being analyzed or modeled. This approach will fail when data representing the nature of a given complex problem does not lend itself to a predetermined functional form and changes behavior multiple times.

Unlike traditional proxy models, data-driven analytics (DDA) takes a different approach to developing proxy models. In this approach, unlike reduced order models, physics and space-time resolution are not reduced and instead of using predefined functional forms that are more frequently used to develop response surfaces, a series of machine learning algorithms that conform to the system theory are used for training, with the ultimate goal of more accurate modeling.

## Unconventional Reservoirs

There is no formal definition of "unconventional resources," despite the fact that unconventional resources are the most active petroleum play in North America. [Meckel and Thomasson \(2008\)](#) defined unconventional resources using purely a permeability threshold ( $< 0.1 \text{ md}$ ). Yet, coal bed methane plays are considered unconventional and many have permeabilities exceeding 1 md over large portions of the fairway (e.g., San Juan Basin and Powder River Basin). Other workers have defined unconventional resources based on an interpretation of the petroleum system and have stated that unconventional resources are "continuous" or "basin centered" and lack traditional traps. While some have restricted the term to product type (i.e., unconventional gas), many shale and tight sand plays have gas, wet gas, and oil fairways and all can be considered unconventional. Heavy oil and oil sands are also unconventional resources and many of these deposits are in reservoirs with permeability exceeding 500 nd. Thus, unconventional resources include both low and high permeability reservoirs with both low and high viscosity fluids. Previous definitions have not accounted for all phases of petroleum in all types of reservoirs in all types of petroleum systems.

All petroleum reservoirs can be plotted on a graph of viscosity vs. permeability (both in log scale) ([Fig. 1](#)). On this graph, conventional resources all plot in the lower right quadrant, regardless of fluid phase. All unconventional resources plot outside this quadrant because of a low ratio of permeability to viscosity. Unconventional resources are thus defined as those petroleum reservoirs whose permeability/viscosity ratio requires use of technology to alter either the rock permeability or the fluid viscosity to produce the petroleum at commercially competitive rates. Conversely, conventional resources are those that can be produced commercially without altering permeability or viscosity. This simple graphical definition avoids the pitfalls inherent in a petroleum system interpretation (i.e., basin centered or self-sourced vs. migrated petroleum). The graphical definition accommodates and delineates tight gas, tight oil, shale gas, shale oil, heavy oil, coal bed methane, and even offshore reservoirs with low k/viscosity ratios.

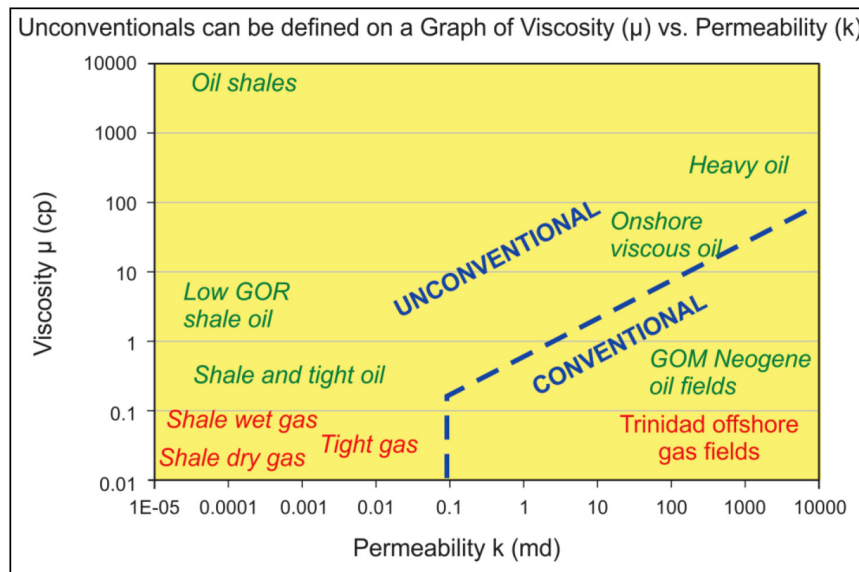


Figure 1—Permeability vs. viscosity for hydrocarbons

## Conventional and Unconventional Resources

Two types of petroleum resources have been defined that might require different approaches for their evaluations:

- Conventional resources exist in discrete petroleum accumulations related to a localized geological structural feature and/or stratigraphic condition, typically with each accumulation bounded by a down dip contact with an aquifer, and which is significantly affected by hydrodynamic influences based on buoyancy of petroleum in water. The petroleum is recovered through wellbores and typically requires minimal processing before sale.
- Unconventional resources exist in hydrocarbon accumulations that are pervasive throughout a large area and that are generally not significantly affected by hydrodynamic influences (also called "continuous-type deposits"). Such accumulations require specialized extraction technology and, in the case of oil, the raw production might require significant processing before sale.

The relationship between conventional and unconventional resources is illustrated by a resource triangle (Fig. 2). Heavy oil and tight gas formations straddle the boundary; nonetheless, both present challenges in applying assessment methods typically used for conventional accumulations.

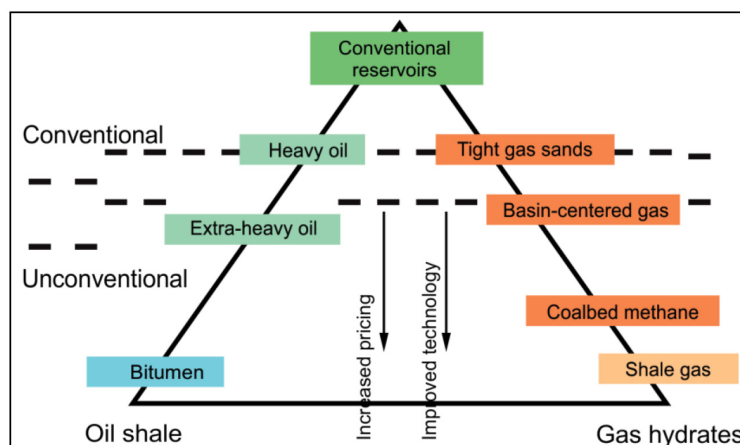


Figure 2—Petroleum-resource triangle

Very large volumes of petroleum exist in unconventional reservoirs, but their commercial recovery often requires a combination of improved technology and higher product prices. Industry analysts project that unconventional liquid reservoirs (excluding oil shale) might contain 5.8 trillion barrels initially-in-place; oil shales might add over 2.8 trillion barrels (WEC 2007). The in-place estimates for unconventional gas accumulations range over 30,000 Tcf (excluding gas hydrates) vs. 2,800 Tcf produced to date (NPC 2007). Estimates for gas hydrates volumes in-place vary widely between 35,000 and 61,000,000 Tcf (EIA 1998); however, no commercial recovery methods have yet been developed to extract these volumes.

It is intended that the petroleum reserves management system (PRMS) resource definitions, together with the classification system (Fig. 3), will be appropriate for all types of petroleum accumulations regardless of their in-place characteristics, extraction methods applied, or degree of processing necessary. However, specialized techniques are often employed in assessing in-place quantities and evaluating development and production programs.

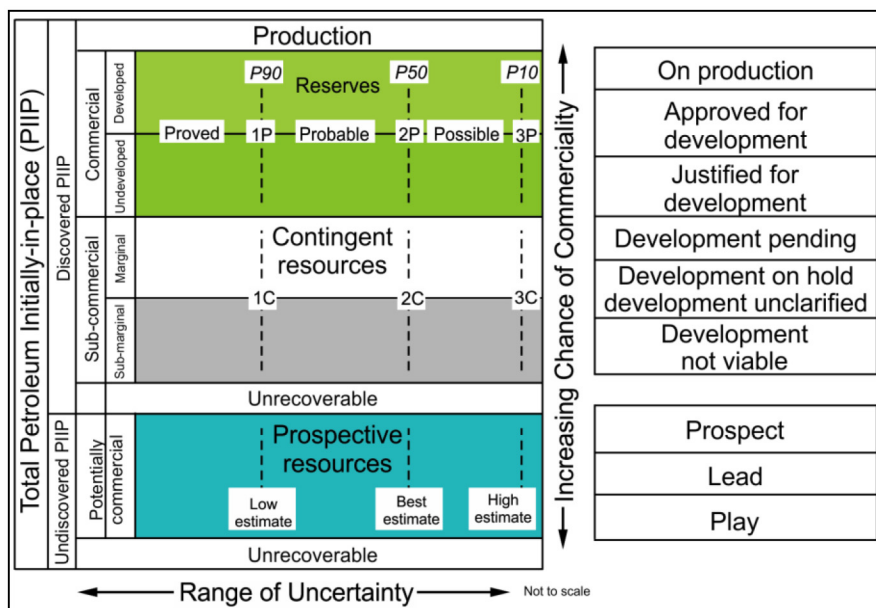


Figure 3—PRMS reserves and resources classification with project maturity subclasses

Estimations of recoverable resource quantities must include an assessment of the associated uncertainty expressed by allocation to PRMS categories using the same low/best/high methodology as for conventional resources. Typically, the evaluation process begins with estimates of original-in-place volumes. Thereafter, portions of the in-place quantities that might be potentially recovered by identified development programs are defined.

As in conventional accumulations, undiscovered recoverable volumes are classified as prospective resources and are estimated assuming their discovery and commercial development. PRMS recognizes that the hydrocarbon type and/or the reservoir quality might not support a flowing well test but the accumulation might be classed as "discovered" based on other evidence (e.g., sampling and/or logging). It is not uncommon to recognize very large areas where prior drilling results have identified the presence of a "discovered" resource type that, based on analogs, has production potential. Where technically feasible recovery techniques are identified but economic and/or other commercial criteria are not satisfied, even under very aggressive forecasts, estimates of recoverable quantities are classified as contingent resources and sub-classified as development not viable. If the recovery processes have been confirmed as not technically feasible, the in-place volumes are classified as discovered/unrecoverable. As the play and

technologies mature and development projects are better defined, portions of estimated volumes might be assigned to contingent resources subclasses that recognize this progressive technical and commercial maturity. Reserves are only attributed after pilot programs have confirmed the technical and economic producibility and capital is allocated for development.

Note that under PRMS, the reserves and resource quantities reported are in the conditions delivered at the custody transfer (sales) point. In many cases, the raw production must be further processed to yield a marketable product. Integrated development/processing projects include the cost of the processing and related facilities in the project economics; in other cases, the raw production is sold to a third party (at a reduced price) for further processing. In either case, development economics are highly dependent on the capital and operating costs associated with complex processing facilities.

The recent emergence of unconventional plays as commercial ventures has brought the realization, that the publicly available literature on standard assessment methods and illustrative examples for unconventional resources is limited. Because these accumulations are often pervasive throughout a very large area and are developed with high density drilling, well productivity is often highly variable. Therefore, probabilistic assessment techniques might be more applicable than in conventional plays.

The PRMS application document provides preliminary information on evaluation approaches used in the following resource types generally referred to as "unconventional:"

- Extra-heavy oil
- Bitumen
- Tight gas formations
- Coal bed methane
- Shale gas
- Oil shale
- Gas hydrates

It is envisaged that these sections will be updated and expanded in future editions as the plays mature and evaluation methods are better defined.

## Process in Evaluating Unconventional Resources

In the exploitation of unconventional resources there are typically four main stages in the assessment process: exploration, evaluation, delineation, and development ([Haskett and Brown 2005](#)). All resource evaluations begin with the identification of hydrocarbons in sufficient quantity to potentially support commercial development. Thereafter, the focus is on identifying the development techniques that can overcome the technical or economic constraints limiting commercial development.

Before the reserves can be estimated and categorized according to the level of certainty, the unconventional resources will need to be classified based on the development project's chance of commercialization. The logic flow based on PRMS classification principles discussed above, are clearly illustrated in [Figs. 4 and 5](#). After the discovered petroleum initially in-place (DPIIP) has been established, the subclassification of contingent resources will be carried out from which different categories will eventually be estimated. Once an economically viable development program has been identified, the company has committed to its implementation and there is a reasonable certainty that any contingencies preventing development will be satisfied, only then can the marketable volumes be reclassified as reserves. PRMS further requires that the development will be normally initiated within a reasonable time frame (e.g., five years); any exceptions must be clearly documented.

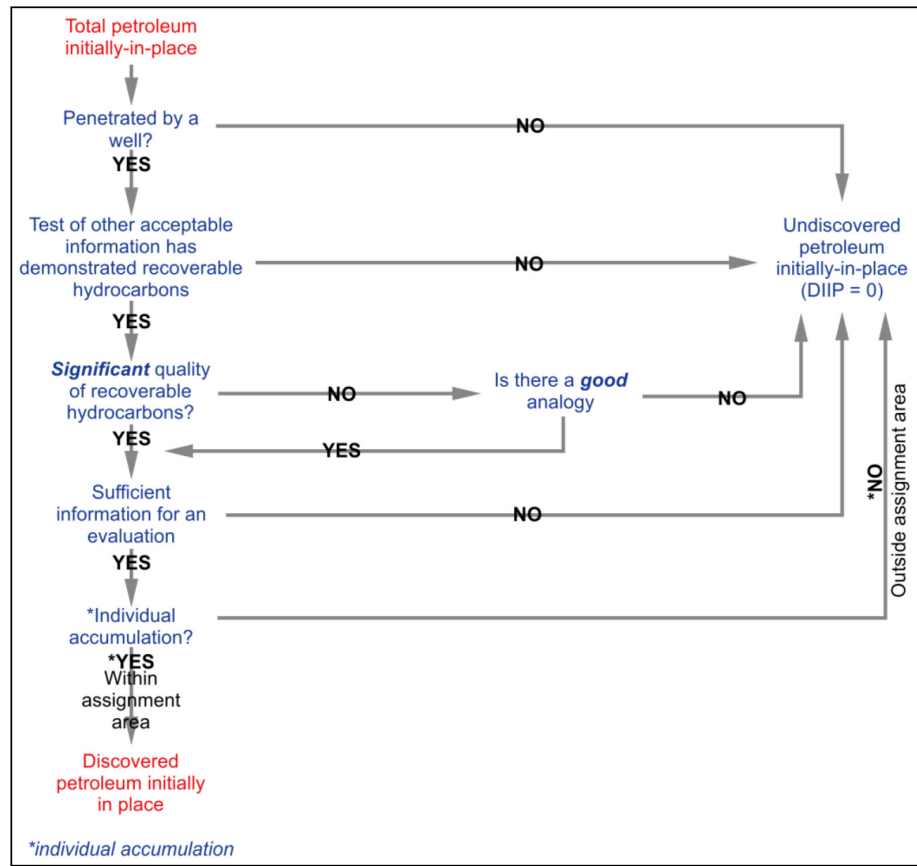


Figure 4—Establishing PRMS total DPIP resources (Elliott 2008)

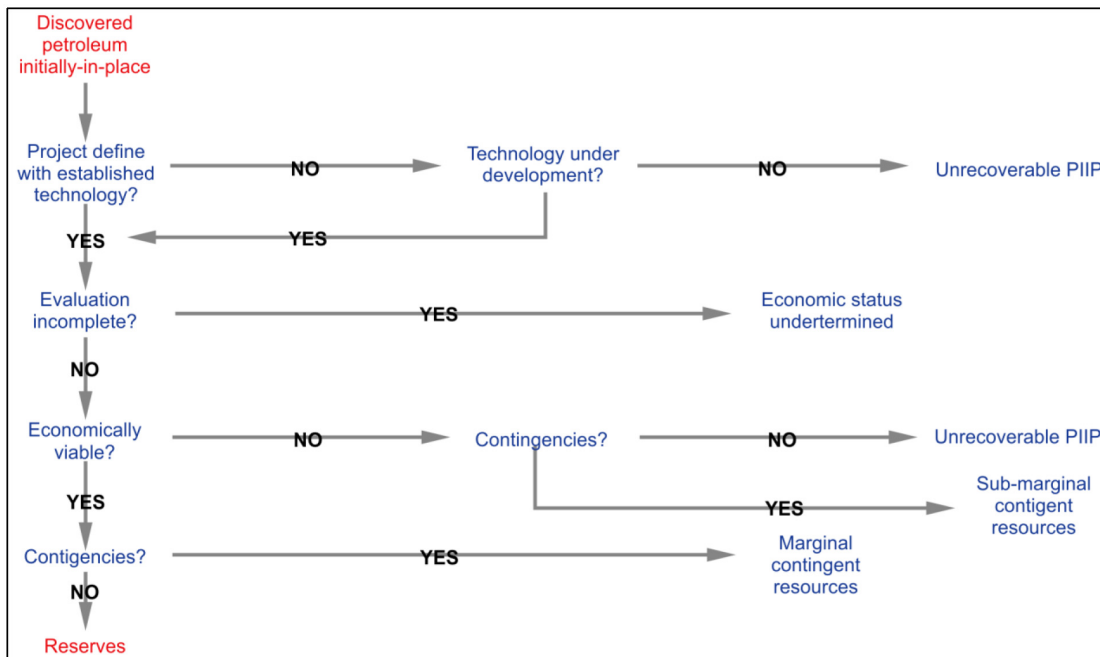


Figure 5—Establishing PRMS contingent resources and reserves (Elliott 2008)

## Stimulation Technologies

### Hydraulic Fracturing

The technique of hydraulic fracturing makes use of a liquid to fracture the reservoir rocks. A hydraulic fracture is formed by pumping the fracturing fluid into the wellbore at a rate sufficient to increase pressure downhole to exceed the strength of the rock.

The term "hydraulic fracturing" is primarily used to refer to the process of fracturing rock formations with water-based fluids. In general terms, hydraulics is a topic in applied science and engineering dealing with the mechanical properties of liquids (not just water). Though there are several definitions, in this note "hydraulic fracturing" was the chosen category to define all techniques that make use of liquids (including foams and emulsions) as the fracturing agent.

Indeed, using water as base fluid for hydraulic fracturing is a more recent development. [Montgomery and Smith \(2010\)](#) provide a good account of the history of hydraulic fracturing.

The first fracture treatments were initially performed with gelled crude and later with gelled kerosene. By the end of 1952, many fracturing treatments were performed with refined and crude oils. These fluids were inexpensive, permitting greater volumes at lower cost. In 1953, water started to be used as a fracturing fluid, and several gelling agents were developed. Surfactants were added to minimize emulsions with the formation fluid. Later, other clay-stabilizing agents were developed, permitting the use of water in a greater number of formations.

Other innovations, such as foams and the addition of alcohol, have also helped enhance the use of water in more formations. Aqueous fluids, such as acid, water, and brines are used now as the base fluid in approximately 96% of all fracturing treatments employing a propping agent. In the early 1970s, a major innovation in fracturing fluids was the use of metal-based crosslinking agents to help enhance the viscosity of gelled water-based fracturing fluids for higher-temperature wells.

**Hydraulic Fracturing of Shales** Shale formations present a great variability, and for this reason no single technique for hydraulic fracturing has universally worked. Each shale play has unique properties that need to be addressed through fracture treatment and fluid design. For example, numerous fracture technologies have been applied in the Appalachian basin alone, including the use of CO<sub>2</sub>, N<sub>2</sub>, and CO<sub>2</sub> foam, and slickwater fracturing. The composition of fracturing fluids must be altered to meet specific reservoir and operational conditions. Slickwater hydraulic fracturing, which is used extensively in Canadian and US (United States) shale basins, is suited for complex reservoirs that are brittle and naturally fractured and are tolerant of large volumes of water.

Ductile reservoirs require more effective proppant placement to achieve the desired permeability. Other fracture techniques, including CO<sub>2</sub> polymer and N<sub>2</sub> foams, are occasionally used in ductile rock (for instance, in the Montney shale in Canada). As discussed in later sections, CO<sub>2</sub> fluids eliminate the need of water while providing extra energy from the gas expansion to shorten the flowback time.

In general, a fracturing fluid can be thought as the sum of three main components:

$$\text{Fracturing fluid} = \text{Base fluid} + \text{Additives} + \text{Proppant}$$

A fracturing fluid can be "energized" with the addition of compressed gas (usually either CO<sub>2</sub> or N<sub>2</sub>). This practice provides a substantial portion of the energy necessary to recover the fluid and places much less water on water-sensitive formations, but have the disadvantage of reducing the amount of proppant possible to deposit in the fracture. Composition of common fracturing fluids is provided in [Table 1](#).

**Table 1—Different fluids used for hydraulic fracturing [adapted and expanded from (EPA 2004; PetroWiki—Society of Petroleum Engineers 2013)]**

Base Fluid	Fluid type	Main Composition
Water based	Slickwater	Water + sand (+ chemical additives)
	Linear fluids	Gelled water, GUAR<HPG, HEC, CMHPG
	Crosslinked fluid	Crosslinker + GUAR, HPG, CMHPG, CMHEC
	Viscoelastic surfactant gel fluids	Electrolyte + surfactant
Foam based	Water based foam	Water and foamer + N <sub>2</sub> or CO <sub>2</sub>
	Acid based foam	Acid and foamer + N <sub>2</sub>
	Alcohol based Foam	Methanol and foamer +N <sub>2</sub>
Oil based	Linear fluids	Oil, gelled oil
	Crosslinked fluid	Phosphate ester gels
	Water emulsion	Water + oil + emulsifiers
Acid based	Linear	—
	Crosslinked	—
	Oil emulsion	—
Alcohol based	Methanol/water mixes or 100% methanol	Methanol + water
Emulsion based	Water-oil Emulsions	Water + oil
	CO <sub>2</sub> -methanol	CO <sub>2</sub> + water + methanol
	Others	—
Other fluids	Liquid CO <sub>2</sub>	CO <sub>2</sub>
	Liquid nitrogen	N <sub>2</sub>
	Liquid helium	He
	Liquid natural gas	LPG (butane and/or propane)

## Pneumatic Fracturing

During pneumatic fracturing, a gas (air, nitrogen, etc.) is injected into the subsurface at pressures exceeding the natural in-situ pressures present in the formation interface and at flow volumes exceeding the natural permeability of the rock.

The pneumatic fracturing procedure typically does not include the intentional deposition of foreign propping agents to maintain fracture stability. The created fractures are thought to be self-propping, a circumstance which is attributed to both the asperities present along the fracture plane and the block shifting, which takes place during injection.

There is no theoretical maximum depth limit for initiating a fracture in a geologic formation as long as sufficient pressure and flow can be delivered to the fracture zone. In pneumatic fracturing the injection pressure necessary to lift the formation is typically two to three times higher than for hydraulic fracturing on account of gas compressibility effects in the system.

Potential advantages:

- Potential environmental advantages:
  - Water usage completely eliminated. No chemical additives are necessary.
- Potential for higher permeabilities attributed to open, self-propelled fractures that are capable of transmitting significant amounts of fluid flow.

Potential disadvantages:

- Limited possibility to operate at depth.
- Limited capability to transport proppants.

## Fracturing With Dynamic Loading

Using explosives to fracture rock formations, and hence stimulate production, is a very old technique. From the 1860s until the late 1940s, explosives were commonly used in wells to increase production (well

shooting). Liquid nitroglycerin in a tin cylinder was lowered down the well and detonated. The technique was both effective and dangerous (Hyne 2001).

### Thermal (Cryogenic) Fracturing

Fracturing can be achieved by using a fluid colder than the reservoir. This will create thermal stresses that could fracture the rock. Even if a fluid is used this is not strictly speaking hydraulic fracturing in the traditional sense, because it is not the elevated pressure of the fluid and high injection rates that breaks the rock.

Several authors (Svendson et al. 1991; Charlez et al. 1996) have shown that thermally induced fractures can take place in oil and gas reservoir stimulation applications. They investigated different cases where cold water was injected into deep hot reservoirs with a constant injection rate (below the formation collapse pressure). After a certain time a sharp increase in injectivity was observed, as if the formation were fractured.

## Fracture Mechanics

Fig. 6 shows hydraulic fracturing is based on the tensile failure mechanism, which can propagate in three ways based on the direction of force applied as given by Griffith (1921).

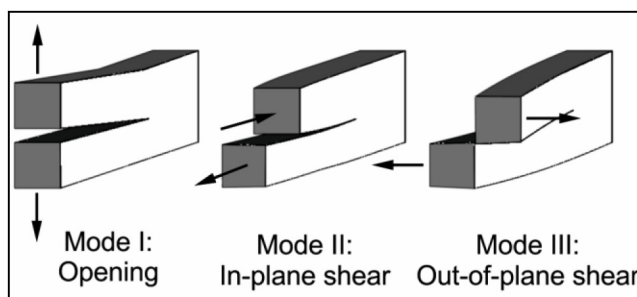


Figure 6—Types of tensile failure (Wikipedia)

*Mode I Fracture*—Tensile stress is acting normal to the plane of the fracture. It can also be defined as opening mode in which width of the fracture increases.

*Mode II Fracture*—This kind of fracture occurs when shear stress is acting parallel to the plane of the fracture and in the direction of a normal to fracture front.

*Mode III Fracture*—Shear stress acting parallel to both the plane of the fracture and the fracture front results in this type of fracture.

### Fracture Initiation and Propagation

Initially pressure induced in the formation of interest is less than the tensile strength of the rock and at this stage the wellbore is intact. Hydraulic fracturing processes in a reservoir can be described by processes explained below, which are the foundation of any numerical or analytical fracture model.

- Once the pressure exceeds the tensile strength of the rock fracture it initiates along a certain direction around the borehole. Once the fracture initiates it can grow or even close depending on the stress state of the formation and property of the fluid after initiation of the fracture initiation models are not valid. Once the fracture initiation starts the process is instantaneous and continuous. Fracture length after initiation is dependent on various factors like rock properties, tensile strength, and fluid pressure. It is evident that in cases of low tensile strength the fracture length is relatively high compared to the formations with high tensile strength.

2. With further increases in pressure and continuous pumping of fluid the pressure builds up until it reaches the fracture propagation pressure. In the vicinity of the borehole, fracture propagation is complex because of stress concentration effects as explained in Balayneh et al. (2004). In near wellbore (NWB) conditions tangential stress is controlled by hoop stress caused by in-situ stress at the tip of the fracture, whereas farther from wellbore fracture propagation is controlled by  $S_{h\min}$  ( $\sigma_h$ ).
3. Once the propagation pressure is exceeded the fracture propagates resulting in the pressure drop attributed to fluid loss and formation of the new fractures.
4. Fracturing fluid reduces the permeability in new fractures and pressure again starts to build up at fracture tips resulting in initiation and propagation of new fractures.

The above steps are shown in Fig. 7; it is also noteworthy that cyclic phenomenon is not observed in case of oil based muds, which is caused by the lack of sand bridging in case of oil based muds, which reduces the fluid loss.

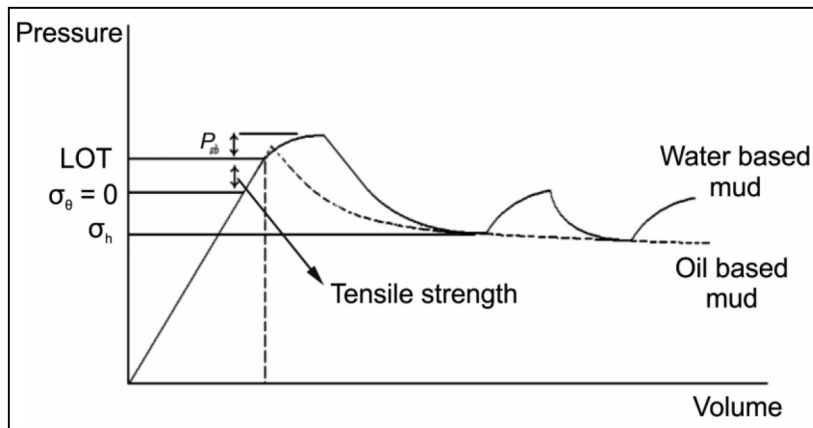


Figure 7—Fracture pressure behavior using oil based mud and water based mud (Kenneth, 2010)

## Fracture Models

Fracture modeling has emerged as a highly complex process considering various physical processes, such as rock properties, reservoir properties, in-situ stress, induced stress, fracturing fluids, and proppant loads etc. Various simulation models are available and deciding a suitable model is an integral part in fracture study. Discrete fracture model and dual porosity/dual permeability model are the conventional models in studying fracture induced production. Dual porosity/dual permeability models consider fractures as homogeneous in nature and simulate a coupling effect of fracture and matrix using equivalent continuum model. These models have high computational efficiency but are limited in terms of fracture shape and flow conditions. This method is inefficient to model small quantity fractures in large stretches and for complex fracture structures. Discrete fracture model (DFM) defines fractures based on actual dimensions and distributions of fractures and assumes Darcy's law for flow through fractures and matrices. Properties and distribution of formation matrix in this method are predefined and are static in nature. Pressure increase NWB caused by long-term waterflooding generally induces dynamic fractures, which over a period of time expand and influence the reservoir performance and sweep efficiency. Conventional models assume fracture length as constant, and thus are unable to simulate such fractures.

Dynamic fracturing modeling is applied to study realistic large scale fractures individually and explicitly. In this method opening and closing of fracture is modeled dynamically by considering permeability and porosity as a function of stress/pressure change.

Recovery from unconventional wells is analyzed using average fracture half length ( $x_f$ ), enhanced reservoir permeability ( $k$ ), and stimulated reservoir volume. For reservoir volume calculation fracture growth modeling is an integral parameter and can be performed using various analytical and numerical models. Miskimins and Barree (2003) approximates the decoupled rock deformation with shear-slip, Daneshy (1978) gives relationship between fracture's propagation and interface bond strength, Warpinski et al. (1982), explains restriction of fracture growth attributed to change in in-situ stress, Barree et al. (2003), showed the influence of interfacial slip on fracture height growth, and Cherian et al. (2014) explains the impact of laminated rock on fracture propagation.

Simulation models are based on several assumptions to render the problem tractable and have been covered in Gidley et al. (1979). Some of these assumptions are elastic formation, plane fracture, symmetric with respect to the wellbore, linear fracture mechanics for fracture propagation prediction, power-law behavior of fracturing fluids, simplification of fracture geometry etc.

Modeling of hydraulic fracturing is completed by coupling fundamental equations of continuity, momentum, and linear elastic fracture mechanics. Relationships between fluid pressure and fracture width are used to integrate fluid flow with material balance to calculate deformation using fracture mechanics. Two dimensional (2D) models solve these complex equations but with limitations stated above. Three dimensional (3D) numerical solutions are less restrictive but are based on assumptions for computational efficiency. Warpinski et al. (1994) compares various simulation methods in detail and classify them based on their complexity, methodology, and rate. Planar 3D models like Terrafrac and HYFRAC3D are considered the most complex models while classical models like Perkins-Kern-Nordgren (PKN) and Greetsma-de Klerk (GDK) are attributed as the least complex models. This paper presents a detailed case study on simulation using a commercial Fracture simulation software and a brief description of some other commercial models is also provided below.

## PKN Model

PKN model (1961) assumes that the fracture height is independent of fracture length and fracture fluid pressure is constant in vertical cross sections perpendicular to direction of propagation. Fracture geometry is assumed elliptical in vertical plane with maximum width in the center and equation for width ( $w$ ) is:

$$w(x, t) = \frac{(1-\nu)h_f(p-\sigma_h)}{G} \quad (1)$$

2D plane-strain deformation in vertical plane is assumed. With a narrow elliptical flow channel and considering flow rate as a function of fracture width, fracture propagation is represented by the following nonlinear PDE:

$$\frac{G}{64(1-\nu)h_f\mu} \frac{\partial^2 w^2}{\partial x^2} - \frac{\partial w}{\partial t} = 0 \quad (2)$$

Where  $G$ ,  $\nu$ ,  $h_f$ ,  $\sigma_h$ , and  $p$  represent shear modulus, Poisson's ratio, major axis of ellipse (fracture height), minimum horizontal stress, and pressure respectively. Boundary conditions for the above equation are:

$$w(x, 0) = 0 \text{ for } t = 0$$

$$w(x, t) = 0 \text{ for } x > L(t) \text{ and}$$

$$q(0, t) = q_i/2 \text{ for two fracture wings}$$

## GDK Model

GDK model is based on Greetsma (1979) and is different from the PKN model because of assumptions in terms of fracture geometry and plane strain condition instead of plane stress. This model assumes fixed

fracture height and with deformation in horizontal plane fracture width is independent of fracture height. The shape of fractures is elliptical in horizontal plane with maximum width at wellbore given as:

$$w(0, t) = \frac{2(1-\nu)L(p_f - \sigma_h)}{G} \quad (3)$$

In case of the PKN method flow rate is function of fracture width, whereas fluid pressure gradient in GDK method is defined w.r.t a narrow rectangular slit of variable width represented as:

$$p(0, t) - p(x, t) = \frac{12\mu q_i}{h_f} \int_0^x \frac{dx}{w^3(x, t)} \quad (4)$$

If one observes the fracture length to be much greater than the fracture height the PKN method is generally recommended and if fracture height is more than fracture length GDK method is usually preferred.

## Planar 3D Models

Major assumptions in such models are planar fractures of arbitrary shape in a linearly elastic formation, 2D flow in the fracture, power-law fluids, and linear fracture mechanics for fracture propagation. TerraFrac and the HYFRAC3D incorporate planar 3D models but are different based on the numerical technique used to calculate fracture opening. Terrafrac uses an integral equation for the fracture opening but Hyfrac is based on a finite-element method. Both models use finite element method (FEM) for 2D fluid flow and fracture tip advancement is proportional to stress intensity factor on fracture tip.

## Planar 3D Finite Difference Models

A description of planar 3D finite difference model, is provided by [Warpinski et al. \(1994\)](#). Fracture opening is calculated by superposition using the surface displacement of a half-space under normal load (Boussinesq solution). It is also assumed that fracture propagates when the tensile stress perpendicular to the fracturing plane exceeds the tensile strength of the formation. This model predicts higher treating pressures and shorter, wider fractures than planar 3D models.

## Pseudo-3D Models

By removing the constant fracture height criteria from PKN model pseudo-3D models are developed. Equations are developed for radial, 2D, and elliptical geometries assuming one dimensional (1D) flow along fracture length. Fracture width is considered as a function of pressure and position and based on that fracture propagation is calculated. These models can be further divided into two categories, one is developed by the dividing fracture along the length into cells and the other is modeled using parametric representation of fracture geometry. Pseudo-3D simulators are computationally very efficient but are limited for geometries matching the PKN model criteria (large length/height). Because of this limitation in complex in-situ stress conditions with unconfined fracture growth a 3D model is more effective.

## Fracture Design and Analysis Software Model

This study presents efficient use of data analytics using the fracture design and analysis software model. The fracture design and analysis software model considers flow rate, rheology of fluid used for fracturing, and proppant concentration to calculate pressure drop in the wellbore. Net fracture pressure and time history of fracture growth are calculated considering non-Newtonian fluid and pressure drop at different proppant phases and entrained proppant. Calculation of fracture dimensions is computationally efficient as the fracture design and analysis software does not calculate point specific variations but uses an integrated approach by considering functional coefficients in governing differential equations. [Hou \(2011\)](#) compares fracture design and analysis software and Flac3D and their merits and limitations. It is evident

that fracture propagation in the fracture design and analysis software is uniform with two half ellipses irrespective of stratigraphy, whereas Flac3D is capable of simulating realistic fracture front. The fracture design and analysis software is also capable of taking proppant transport, fracture closure, and proppant setting into consideration presented in this paper but these features are not available in Flac3D.

Unconventional reservoirs can store huge amounts of oil or gas; however, the matrix characteristics are poor for conventional production solutions. Therefore, well stimulation plays a key role for these reservoirs to achieve an efficient, economical production.

Extra heavy oil reservoirs and oil sands (bitumen containing sands) have fluid with high viscosity and low API gravity ([Cupcic 2003](#)). Production from these reservoirs is largely dependent on the thermal stimulation processes to reduce viscosity and large pressure drops to induce flow. Cyclic steam stimulation (CSS), steam flooding, wet or dry in-situ combustion with air or oxygen injection or the combination of these methods are older methods. Currently using methods for extra heavy oil reservoirs are CSS, steam assisted gravity drainage (SAGD), vapor assisted petroleum extraction (VAPEX), and toe-to-heel air injection (THAI).

Other methods like solvent injection, biological methods, cold gas injection ( $\text{CH}_4$ ,  $\text{CO}_2$ , etc.), polymer methods and in-situ emulsification methods are currently being researched to optimize the recovery; however these methods have not proved viable for heavy oil ([Reinhardt 2010](#)). In-situ combustion method has also not proved economically viable yet.

CSS consists of three stages, steam injection, soaking, and production. Methods can be applied in vertical, deviated, and horizontal wells. The method consists of three stages as injection steam, soaking, and production. By heat introduced to the formation, viscosity reduction is aimed. This method is successfully used for various fields globally, Venezuela, Alberta, Canada etc.

Steam assisted gravity drainage is one of the most recently used methods to produce heavy oil. The method uses a pair of parallel horizontal wells. The upper well involves high pressure steam injection to reduce the oil viscosity and mobilize the oil and gravity segregation for flow to the lower production well ([Butler 1998](#)). The method is widely used in Alberta, Canada to recover tar sands and heavy oil reservoirs.

VAPEX is like the SAGD process but it consists of injection of light hydrocarbon vapors or their mixtures with noncondensable gases instead of steam to reduce the viscosity through sufficient solvent dissolution and possible asphaltene precipitation. The method conducted via a pair of horizontal wells, which are positioned with an appropriate vertical distance inside the reservoir ([Rahnema et al. 2008](#)). A gaseous solvent mixture injected through the upper well and the solvent gradually dissolved in the heavy oil and oil viscosity reduction is provided. The solvent diluted heavy oil drained to the lower production well by gravity ([Rahnema et al. 2008](#)).

However, for tight gas, coal bed methane and shale gas reservoirs; fracturing is the main tool to develop these reservoirs. Because these reservoirs have very low permeability, stimulation techniques are needed to create flow paths and to ease fluid flow; as a consequence have a best early production rate and the highest ultimate recovery ([Zahid et al. 2007](#)).

Tight gas reservoirs can be defined mainly as low-permeability reservoirs, which mainly produce dry gas. Holditch (2006) defines the tight gas reservoirs as, "The reservoirs that cannot be produced at economic flow rates nor recover economic volumes of natural gas unless the well is stimulated by a large hydraulic fracture treatment or produce by use of horizontal wellbore or multilateral wellbores." The same definition can be used for all the unconventional resources. Primary aim of stimulation treatment is to provide a conductive path for flow and by lateral wells increase the contact area for the production ([Saldungaray et al. 2013](#)). The optimum design of drilling, completion, and stimulation methods depend on the reservoir characteristics and economics. Early attempts for developing tight gas reservoirs end up with very poor flow rates and rapid declines. In general the key production method for these reservoirs was locating the well to the areas where the natural fractures exist in early attempts ([Zahid et al. 2007](#)). If the natural fractures are scarce, the wells needed to be stimulated. Now, technologies like multistage

fracturing, high-efficiency fracture fluids, and light weight mono-layer proppants have proved their capability to help enhance productivity and recovery from tight gas reservoirs ([Zahid et al. 2007](#)). In many countries, Canada, Australia, Mexico, Venezuela, etc. have production from tight gas reservoirs.

Recent well drilling, completion and stimulation technology advancements used in shale/tight gas reservoirs have led to transfer the technology for shale and tight oil reservoirs. Unconventional light oil reservoirs can be classified into three groups according to their properties. [Clarkson and Pederson \(2011\)](#) have a classification of these reservoirs based on flow characteristics as: Halo oil: light oil plays where the source and reservoir are not the same and matrix permeability is relatively high. An example of this kind of play is Cardium and Viking pools in Alberta. Tight oil: light oil plays where the source and reservoir are not the same but matrix permeability is low (<0.1 md). These plays are analogous to the tight gas plays. Examples of this kind of play are Saskatchewan Bakken formation and some parts of Montney in Alberta. Shale oil: where the source and the reservoir are the same, matrix permeability is very low, and organic content can be high and these plays are analogous to shale gas plays. Examples of this kind of play are second White Speckled Shale, Duverney, and Muskwa shales. These shales are also distinguished from shale oils, which are needed in thermal stimulation ([Clarkson and Pedersen 2011](#)).

For tight oil reservoirs fracturing horizontal wells stimulated with slick water or hybrid techniques is the most common method to produce these reservoirs ([Williams-Kovacs and Clarkson 2013](#)).

Coal bed methane also known as coal seam gas (CSG) is naturally occurring methane contained in the coal seam as a result of chemical and physical processes during the coal formation. Coal has an enormous amount of surface area and can hold large quantities of methane. Methane absorbed to the surface of the coal is a known fact from the early times of the coal mining practices. Hydrostatic pressure causes methane to adhere to the coal surface by adsorption. Most of the methane stored in the molecular structure of the coal as an absorbed state, some is stored in the fractures or cleats as free gas or dissolved in the water trapped in the fractures ([National Energy Technology Laboratory 2003](#)). The sorption isotherm defines the relationship of pressure to the capacity of a given coal can hold gas at a constant temperature. When the reservoir pressure drops, methane desorbs off the coal surface, diffuses through the matrix material, and flows through the natural fracture system of the coal (cleat system). Cleat system consists of two orthogonal sets of fracture systems called face and butt cleats. Face cleats are continuous throughout the system, while butt cleats are discontinuous and generally orthogonal to the face cleats. Generally, maximum permeability direction is assumed in the direction of face cleats ([Vishnukumar 2007](#)). Coal cleat systems are generally saturated with water; therefore gas can only be mobilized by decreasing the hydrostatic pressure in the coal seam by initial dewatering. Once water is removed from the system, gas desorbed from the surface of the coal structure and forms a free gas phase in the cleat systems. Initial flow rates from these wells are generally very low. To enhance gas rates and accelerate desorption, stimulation techniques are used.

Openhole cavity completion has recently been mentioned as an alternative method to hydraulic fracturing in coal gas wells ([Goktas and Ertekin 1999](#)). Cavity completion is a consequence of enlarging openhole interval by injecting air or air-water mixture at a high pressure and then releasing the wellbore pressure suddenly (surging). This sudden pressure decrease causes friable, weak coal, and rock particles to slough into the wellbore. The injection and surging phases are repeated until the cavity is stabilized and the wellbore is free of debris. In this process it is assumed that tensile and shear fractures achieved as a result of sudden increase and decrease of the wellbore pressure. Tensile fractures are created during the injection process because of higher wellbore pressure than minimum in-situ stress and shear fractures are created as a result of sudden reduction of wellbore pressure. Accordingly, high density fracture network around the wellbore is created as a result of this process. Moreover, because of slough of NWB rock into the wellbore, possible drilling damage is removed and wellbore diameter is enlarged ([Goktas and Ertekin 1999](#)). This method was used in San Juan Basin in Fruitland coal and best results are achieved in the over pressured and high permeability areas of the basin.

Hydraulic fracturing in coal bed methane reservoirs aim to connect the natural fracture system (cleat system) with the wellbore and accelerate desorption. It is the most common stimulation technique used for CBM wells.

In lower pressure, high  $kh$  CBM reservoirs, water enhancement treatment is a sufficient way to stimulate the well. In this process pumping water is produced at a high rate for instance 0.5 to 1 bbl/min/ft of coal of approximately half an hour. This treatment aims to clean out the plugged cleats NWB and decrease the skin effect. The best example for this treatment is Wyoming, Powder River Basin Ft. Union coals (Cramer 2008).

Some of the CBM reservoirs are already dewatered and directly produce dry gas. In these reservoirs best working stimulation treatments are based on  $\text{CO}_2$  and  $\text{N}_2$  treatments (Cramer 2008). One of the examples for this kind of stimulation is Nitrogen stimulation for instance is Horseshoe Canyon in Alberta and has been stimulated effectively with coiled tubing (CT)-isolated  $\text{N}_2$  fracturing (Settari et al. 2010). The technique consists of isolating and sequentially treating individual coal seam with high rate nitrogen fracturing without proppant (Rieb and Leshchyshyn 2005).

Recently a study was conducted on the cryogenic nitrogen as a fracturing (McDaniel et al. 1997). According to McDaniel et al. (1997) this technique involves delivering liquefied nitrogen to a moderate-depth formation at a typical fracturing rate at cryogenic temperatures (-320°C to -232°F). With this method a high degree thermal shock introduced to the system and this shock creates physical alteration of the fracture walls to prevent closure of the hydraulically or thermally induced fractures. However, this method has not yet viable (McDaniel et al. 1997).

Another newly used method for fracturing a coal seam is a low polymer concentration crosslinked fracturing. The best usage of these fracturing fluid systems is in higher energy reservoirs, which have high reservoir pressure and moderate to high permeability (Cramer 2008). In San Juan Basin, Ft. Union and Mesaverde formations this method was applied successfully (Cramer et al. 2004).

The commercial fracturing simulator uses the following models as excerpted from its technical manual for fracture geometry and proppant transport. Inputs are varied over a range to produce different outputs and then to use in the data analytics to see the impact and relationship between the inputs and the outputs on the recovery.

## Fracture Geometry Model

The hydraulic fracture module is 3D in that spatial variations in reservoir stress, modulus, pressure, and flow distribution are considered. However, it does not need to calculate the variations at specific points within the hydraulic fracture. Instead, the effects are integrated into functional coefficients of the governing differential equations, which greatly simplify the calculations of hydraulic fracture dimensions. The module can therefore run several times faster than real time, which is necessary for history matching of measured net pressure. The coefficients necessary to calculate the spatial variations are obtained from a fully 3D model and checked against experimental and field test data. Simulator handles up to 100 layers to define the reservoir(s) and surrounding formations.

The basic techniques employed in the 3D lumped fracture models are described in Crockett et al. (1986). However, numerous changes and clarifications have been achieved since that paper was written, and those are reported here.

The easiest way to present these modifications and resulting structures in **Simulator** is in terms of the shape factors  $S_{Ti}$  (where  $T$  represents the type of mechanism) multiplying the basic propagation coefficients  $\gamma_{i2}$  in Eq. 13b of Crockett et al. (1986) as represented below:

$$\gamma_2 = \gamma_2 S_{ki} S_{Si} S_{di} S_{pi} S_{pi} S_{Li} \quad (5)$$

where  $i=1, 2, 3$  correspond to length, upper, and lower height, respectively. The subscripts K, S, d,  $\mu$ , p, and L correspond to hydraulic fracture, stress, deformation modulus, viscosity, proppant, and leak-off mechanisms, respectively.

In addition, The Beta-coefficients are used, associated with the shape-factors in Eq. (5) allow a major flexibility in the ability of **Simulator** to accept/represent ongoing research results (for example from **R3DH**). These beta-coefficients are represented as BETA (I, J, and K) in the **Simulator** code and are available as background menus for researchers within companies using **Simulator**.

## Shape Factors for Fracture Toughness

One major issue that has been raised continuously was the role of hydraulic fracture toughness  $K_c$  in hydraulic fracture propagation. There is no explicit account of toughness in Crockett et al. (1986), based on the many previous arguments showing it to have a negligible effect in typical large scale operations. However, to allow handling of small -scale hydraulic fractures, such as those induced during stress testing, and also to allow comparison with equivalent hydraulic fracture toughness (e.g., Eq. 5), an explicit incorporation of  $K_c$  has been achieved with a shape factor:

$$S_{Ki} = \text{MAX}[0, 1 - K_c \beta_K / (\sigma \pi l_i)]^{1/2} \quad (6a)$$

The characteristic lengths  $l_i$  depends on the dimension being propagated (in accordance with  $\gamma_2$  above) and the geometry of the hydraulic fracture; to determine them, one as to make adaptations of standard formulae from hydraulic fracture mechanics:

$$l_i = [(L_2 + L_3)/2]^{I+1}/L^I E(\kappa); \kappa^2 \equiv 1 - (L_2 + L_3)^2/4L^2 \quad (6b)$$

with  $I=1$  when  $i=1$ ,  $I=0$  when  $i=2, 3$ .  $E(\kappa)$  is the complete **Elliptic Integral**.

The coefficient  $\beta_K$  is used to allow some flexibility in weighting the stress -intensity factor K produced by the pressure distribution associated with  $\sigma$ .

## Shape Factors for Stress Variation

Crockett et al. (1986) defined how stress calculations could be included in the calculation of shape factors. These have also been modified and expanded in numerous important ways. The most important might be to allow multiple layers for stress, modulus and permeability. To achieve this, the functions appearing in the shape factors Eq. 6b must be generalized as follows:

$$S_{Si} = \left[ \sigma - \sum_{h_i=L,3}^{L,2} f_{skli} \Delta \sigma_{sh_i} \right] / \sigma \quad (7a)$$

$$S_{Si} = \left[ \sigma - \sum_{h_i=1}^M f_{skli} \Delta \sigma_{sh_i} \right] / \sigma, i = 2, 3 \quad (7b)$$

in which the current location of the hydraulic fracture perimeter is located by  $L_1$  and heights

$$H_{L2} < L_2 < H_{L2+1}, H_{L3} < L_3 < H_{L3+1} \quad (7c)$$

The functions  $f_{skli}$  resemble those defined by Crockett et al. (1986), except that some simplifications and more effective generalizations have been achieved, as follows:

$$f_{sil1} = f_1(H_{L1}/l_1) \exp[(\beta_{si}-1)f_2 - (H_{L1}/L_1)] \quad (7d)$$

$$f_1(h) \equiv 1 - 2 \arcsin(h)/\pi, f_2 \equiv 1 - f_1 \Delta \sigma_c / \sigma \quad (7e)$$

An equilibrium height is achieved in the special case of  $f_2=0$ , but that  $\beta_{Si}$  can serve as a control knob to increase ( $\beta_{Si} > 1$ ) or decrease ( $\beta_{Si} < 1$  s barriers), even in the special cases where such an equilibrium

height exists. The values of  $\beta_{S_2}$  and  $\beta_{S_3}$  might be observed by varying J (the switch) one allows the options of extreme containment, normal growth [for example from R3DH (Cleary et al. 1988)] and lab experiments Johnson 1990), or very little containment in either direction; these options allow the representation of alternative mechanisms, such as containment by slippage at interfaces (e.g., Lam and Cleary 1985), which was chosen to not incorporate in explicit parametric terms, because of poor potential to measure the necessary parameters.

The other functions  $f_{s_{111}}$  are for convenience, chosen in relation to the upward and downward growth functions in Eqs. (7e and f). Specifically, the length of growth is tied somewhat to vertical growth:

$$f_{sil1} = f_1(H_{11}/l_1)[1 - \exp\beta_{S1}(1 - L_i/H_{11})] \quad (7f)$$

but with another Beta-coefficient  $\beta_{S1}$ , which allows variable degrees of coupling between lateral and vertical growth:  $\beta_{S1}$  is observed in the BETA (1, J, and 2) slot of Table 1 and can vary from infinity (that is length of growth follows the average height growth when  $\beta_{S1}=1$ ) to zero, when the length growth is unaffected by stress barriers.

## Fracture Width and Cross-Sectional Profiles in Stress Layers

Lastly, the crack-opening functions  $S_S$  (and  $S_g$ ) also contains functions, which bear a relationship with  $f_{sil1}$ , but this correspondence is more of a coincidental nature:

$$f_{sol1} = f_1(h_{11})/2 - h_{11}\ln\{[1 + (-1)^i(1 - h_{11})^2]^{1/2}\}/h_{11}/\pi. \quad (7g)$$

$$f_{gol1} = 1 + (2 - \pi)\exp[-\beta_c(R_{11} - 1)], R_{11} = L_{11}/h_{11}H \quad (7h)$$

$$h_{11} = [H_{11} - (-1)^i H_D]/H, 2H \equiv L_2 + L_3, H_D = (L_2 - L_3)/2 \quad (7i)$$

Which represents the effects of pinching on the crack-opening at the middle of the perforations—which might, or might not, coincide with the middle of the pay zone [Crockett et al. (1986) is applicable only to a symmetric three-layer system and Eq. 7g specializes to those defined for that case].

Recognizing the issue of pinching at all points along the hydraulic fracture, and especially in light of various claims that pinching could dominate proppant transport (for instance), one has also derived a more general set of formulae, which can be used to approximately represent the hydraulic fracture opening,  $\delta$ , at any point along a vertical cross-section at the wellbore (from which Eqs. 7g through i derive as special cases):

$$\begin{aligned} \pi \bar{E} \delta(h)/H &\approx \gamma_1^c \sqrt{1-h^2} \left( \sigma - \sum_{i=1}^{L2} f_1(h_i) f_{gol1} \Delta \sigma_{oi}/2 \right) \\ &- \sum_{i=L3}^{L2} (h_i - h) \operatorname{arccosh} \left[ \frac{1 - h_i h}{|h - h_i|} \right] \Delta \sigma_{oi} \end{aligned} \quad (7j)$$

It represents the point of interest with dimensionless location

$$h \equiv [z - (-1)^i H_D]/H \quad (7k)$$

and  $\gamma_1$  is the crack-opening coefficient for uniform stress.

## Shape Factors for Modulus Variation

A similar procedure can now be adopted for the effects of modulus stratification:

$$S_d = \prod_{i=-L3}^{L2} f_{di}(e_{ti}) \quad (8a)$$

$$S_{di} = \prod_{l_i=-1,3}^{L_2} f_{dil_i}(e_{l_i}) e_{l_i} = \bar{E}/\bar{E}_{l_i} \quad (8b)$$

in which the functions in the shape-factors  $S_d$  and  $S_{di}$  take a form analogous to those defined by Crockett et al. (1986):

$$f_{dl1}=e_i+(1-e_{l1})\exp(-\beta_d L_i H_{l1}) \quad (8c)$$

$$f_{dl1}=1+(f_{dl1}-1)\exp(-\beta_d L_i H_{l1}) \quad (8d)$$

These exponential functions are chosen so that the multiplying factor  $S_d$  changes the crack-opening coefficient  $\gamma_1$  from the value (for example,  $\gamma_1$ ), associated with a uniform modulus  $E$ , to the extreme of  $E/E_{il}$ , which would govern if  $E_{il}$  persisted; the exponent  $\beta_d$  can be observed in the slot for BETA (0, J, and 3)—again allowing extremes to be explored, on either side of a normal value (that is using J=0, 1, and 2).

However, the behavior of  $f_{dl1}$  is not as easy to identify, except that they certainly should go from unity for small  $L_i/H_{l1}$  back to unity for large  $L_i/H_{l1}$ . Only detailed runs with the hybrid code SIFEH (Keat et al. 1988), coupled to R3DH (Cleary et al. 1988), will allow one to get better forms than those in Eq. 8d; meanwhile, it is recommended that the use of  $\beta_{di}=\infty$  for i=1, 2, and 3, that is for BETA (I, J, and 3), I=1, 2, and 3.

## Shape Factors for Viscosity, Proppant, Temperature, and Radial Weighting

The formula provided in Crockett et al. (1986), expresses the fact that temperature of the fluid varies from that in the wellbore  $\theta_w$  to that in the reservoir  $\theta_R$  as fluid enters and follows the main hydraulic fracture: the associated characteristic dimension  $L_\theta$ , over which the heat-up occurs, is observed to be quite short-of order tens of meters-so that the fluid quickly goes to reservoir temperature in most large-scale treatments. This effect might be partly responsible for the observation, which one has made on (almost) all field data-sets: the injection of a viscous pad after a thin fluid (for example KCl water) seems to produce very little rise in net pressure, that is the viscous fluid might be quickly degraded. An additional major (probably dominant) factor in this observation is the leading-edge behavior, which has been observed in laboratory experiments (Johnson 1990) and analyzing with R3DH Cleary et al. 1988). To capture both effects, it has been introduced as a radial weighting function  $f(r/R)$  for the effects of the many possible viscosities in the hydraulic fracture:

$$\bar{\mu}_i = \sum_{m=1}^M \bar{\mu}_{mi} \left[ L_{mi} f\left(L_{mi}/L_{m}\right) - L_{(m-1)i} f\left(L_{(m-1)i}/L_{m}\right) \right] \quad (9a)$$

$$f(x) \approx [1 - x^2] \beta_{RV} \cdot \bar{\mu}_{mi} = \bar{\mu}_{mi}^v - (\bar{\mu}_{mi}^g - \bar{\mu}_{mi}^s) \exp(-\beta_{VT} L_\theta / L_{mi}) \quad (9b)$$

in which  $L_{mi}$  are the dimensions of the various fluid stages (see Eq. 1). The beta-coefficients  $\beta_{RW}$  and  $\beta_{VT}$  might be observed in the slots allocated to BETA (I, J, and 4), again allowing various extremes for J=0, 1, and 2.

In addition, one can capture the effect of proppant on fluid drag by writing an equivalent viscosity, which depends on proppant concentration, for example:

$$\bar{\mu}_{mi}^v = \bar{\mu}_{mi}^w \exp(-\beta_{VP} \phi_p / \phi_{pp}) \quad (10)$$

in which the  $\beta_{VP}$  are recorded in the slots BETA (I, J, and 5) of Table 1.  $\phi_p$  is the volume concentration of proppant and  $\phi_{pp}$ s the packed-bed value of  $\phi_p$ .

## Shape Factors for Leak-Off

These factors were not defined in Crockett et al. (1986). Functions are now defined as being associated with these shape factors, allowing for the possibility of multiple permeability layers, namely

$$S_{L_i} = \beta_{L_i} \frac{\sum_{l=1}^{L_i-1} k_{ll} (H_{l_i} - H_{l-1}) \gamma_{Al_l} / \sqrt{t - t_l} + k_{l_i} (L_{l_i} - H_{l-1}) \gamma_{Al_l} / \sqrt{t - t_l}}{k \sum_{l=1}^{L_i-1} (H_{l_i} - H_{l-1}) \gamma_{Al_l} / \sqrt{t - t_l} + (L_{l_i} - H_{l-1}) \gamma_{Al_l} / \sqrt{t - t_l}} \quad (11a)$$

in which the average permeability is defined

$$\bar{k} = \frac{\sum_{l=1}^{L_i-1} k_{ll} (H_{l_i} - H_{l-1}) \gamma_{Al_l} + k_{l_i} (L_{l_i} - H_{l-1}) \gamma_{Al_l}}{\sum_{l=1}^{L_i-1} (H_{l_i} - H_{l-1}) \gamma_{Al_l} + (L_{l_i} - H_{l-1}) \gamma_{Al_l}} \quad (11b)$$

in which the beta-factors  $\beta_{L_i}$  are recorded in the slots associated with BETA (I, J, and 6) of Table 1 and  $\gamma_{Al_l}$  are equivalent loss-area factors.

Again the lengthwise growth factor is expressed as a suitable average of the height growth factors, namely

$$S_L = (S_{L_2} + S_{L_3}) / 2 \quad (11c)$$

The propagation rate  $L_i$  is now obtained using methods defined by Crockett et al. (1986) but those equations are also redefined and generalized.

## Proppant Transport Model

**Simulator** models the convection of proppant in a hydraulic fracture. Initial laboratory and computer simulations indicate that proppant convection might be a dominant mechanism in propped-fracture stimulations. **Simulator** also models proppant settling considers the effects of non-Newtonian fluids, hindered settling rates, and settled bank buildup.

The basic methodology for the tracking of proppant stages is to employ mass-conservation as the primary equation for the outside dimensions  $L_{im}$  of the  $M_{th}$  stage

$$W_m - W_{Lm} = \rho_m \gamma_{Vm} V_m \Delta m (L_2 m + L_3 m) L_1 m \quad (12)$$

in which  $W_m$  is the material mass injected since the beginning of stage  $m$ ,  $W_{Lm}$  is the mass of fluid lost from all stages since (and including) stage  $m$ , and  $\rho_m$  is the overall average density of the remaining material. The volume factors  $\gamma_{Vm}$  are intended to allow distortions of the shapes associated with various stages and  $\Delta m$  are the effective widths: if  $\Delta m$  is equated with  $\Delta$  in the corresponding overall mass conservation, then  $\gamma_{Vm}$  represents both perimeter shapes and width distribution for the mass injected since the beginning of stage  $m$ .

To model proppant bank formation, attributed to dehydration and/or bridging, it is necessary to track the material exchange between stages caused by settling and also the fluid leak-off to the formation. The result is a two-part expression for the change in proppant concentration  $\rho_{pm}$  associated with each stage; as well, because settling and dehydration are different for the upper and lower segments of the hydraulic fracture, one must differentiate between upper concentration  $\rho_{pm2}$  and lower concentration  $\rho_{pm3}$ . The resulting expressions for variations in concentrations are then as follows, for each stage (volume  $V_m$ ):

Because of settling of proppant:

$$V_{mi} \dot{\rho}_{pmi}^s = [A_{pm} v_{SM} \rho_{pm} - A_{Oid} v_{SOM} \rho_{Oid}] \quad (13a)$$

because of the influx of proppant, caused by settling velocity  $v_{SI}$ , with effective concentration  $\rho_I$  through an upper influx area  $A_I$  countered by outflux of proppant, caused by settling velocity  $v_{SO}$ , with effective concentration  $\rho_O$  through a lower outflux area  $A_O$ . The settling velocity  $v_S$  also had to be corrected (or at least clarified) from that defined by Crockett et al. (1986), namely:

$$v_S = (2n+1)d [(\rho_p - \rho_f)gd/6K]^{1/n} / (9n) \quad (13b)$$

with  $v_S$  in **the same units as d/time..** In addition, there is a variation of proppant concentration attributed to leak-off:

$$\dot{\rho}_{pmi}^L = \rho_{pmi} [\dot{W}_{Lmi} - \dot{W}_{L(m-1)}] / [W_{mi} - W_{Lmi} - W_{(m-1)i} + W_{L(m-1)i}] \quad (14a)$$

in which the leak-off rate associated with each stage and segment  $W$  must be calculated, for example in relation to the overall leak-off  $W_L$ . A variety of approximations can be used to achieve this, but one has tried to achieve the most generality without great loss of accuracy and computational efficiency, which have been the hallmarks of **Simulator**. In particular, in reference to Eq. 2, the leak-off associated with the group of stages beginning with stage  $m$ , as follows:

$$(kAt)_{mi} \equiv \left[ \sum_{l_1=1}^{l_1-1} k_{l_1} (H_{l_1} - H_{(l_1)i}) \right]_{mi} L_{mi} \gamma_{Ami} \quad (14b)$$

$$+ k_{Li} (L_{mi} - H_{Li}) t_{mi}^{-H_{Li}} \leq L_{mi} \leq H_{Li+1}$$

Using the geometry of Eq. 2 and the times  $t_{mi}$  elapsed because stage  $m$  reached the  $(l_1)^{\text{th}}$  permeable layers, one can calculate the leak-offs associated with each segment:

$$W_{Lmi} \approx W_{Li} [(kAt)_{mi} / (kAt)_i]^{1/2} \quad (14c)$$

A commercial fracture simulator has been used in this study. The inputs are listed below with screenshots. The relationship has been investigated between the inputs below and the output as cumulative production.

- Fracture half length (ft)
- Lifetime PI ratio
- Fracture height (ft)
- Fracture top (ft)
- Fracture bottom (ft)
- Payzone coverage ratio (%)
- Average fracture conductivity (md-ft)
- Average proppant concentration (lb/ft<sup>2</sup>)
- Slurry volume (bbl)
- Prop total (klb)

## Results and Discussion

As far as the relative importance of variables is concerned; fracture half-length is very significant where fracture bottom has more significance than that of fracture top in this specific case. Total proppant used has similar significance as fracture height. Pay zone coverage, slurry volume, and average fracture conductivity have similar amounts of significance. The cause-effect (input-output) relationship is shown above for each parameter in Figs. 8 through 16.

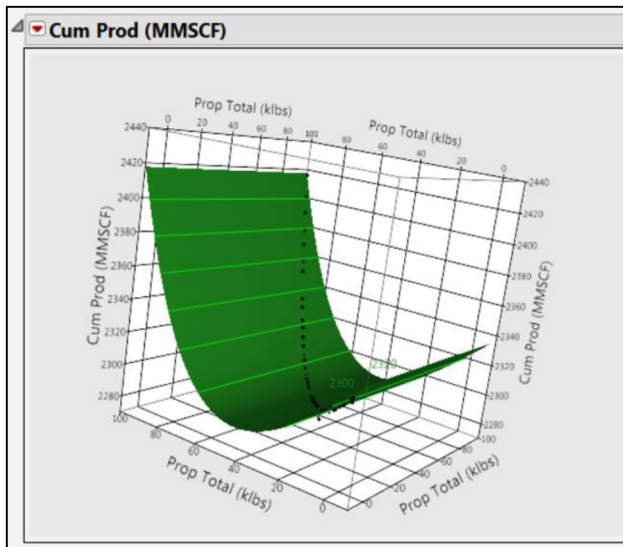


Figure 8—Prop. total vs. cumulative production

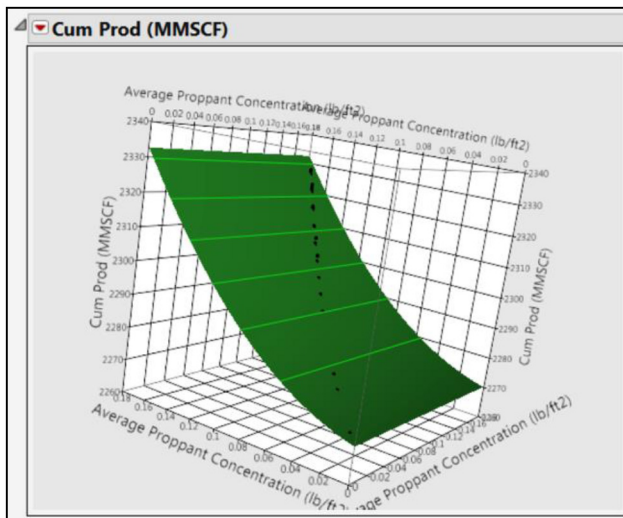


Figure 9—Average prop. concentration vs. cumulative production

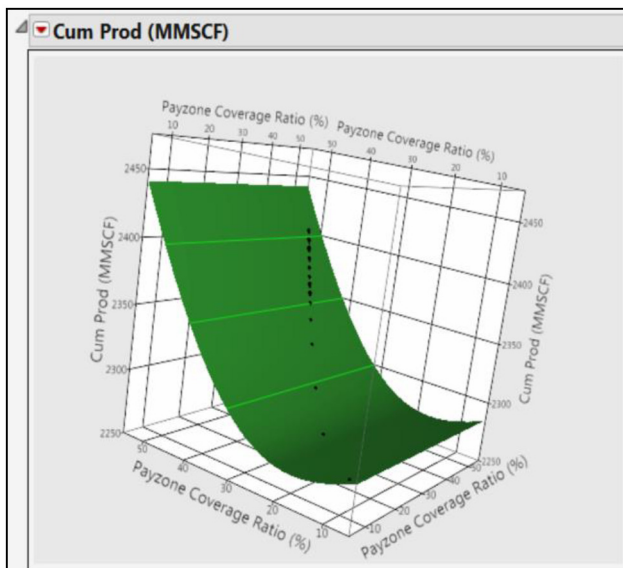


Figure 10—Fracture bottom vs. cumulative production

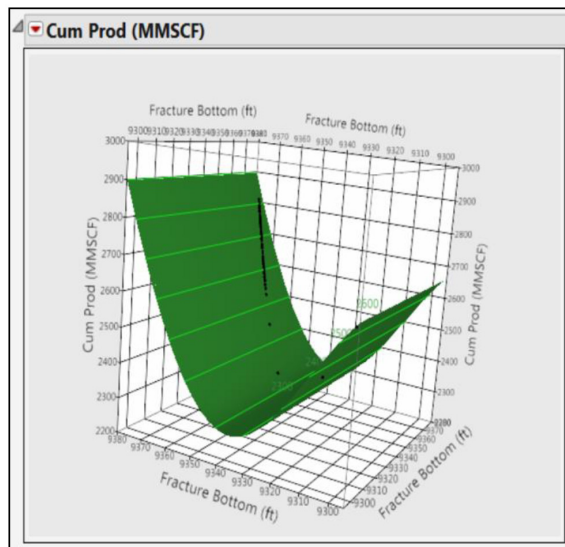


Figure 11—Payzone coverage ratio vs. cumulative production

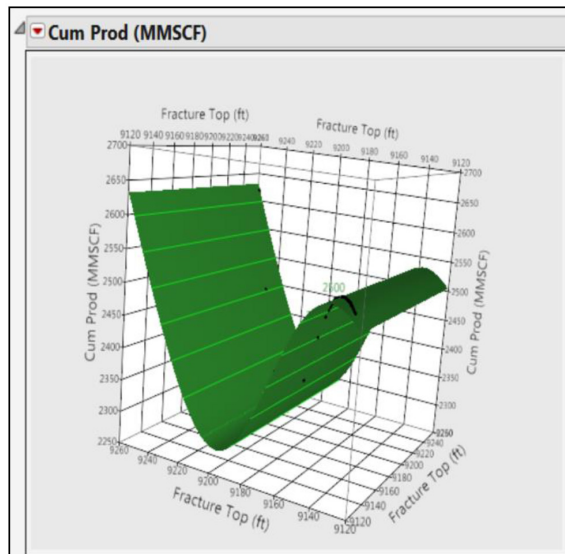


Figure 12—Fracture top vs. cumulative production

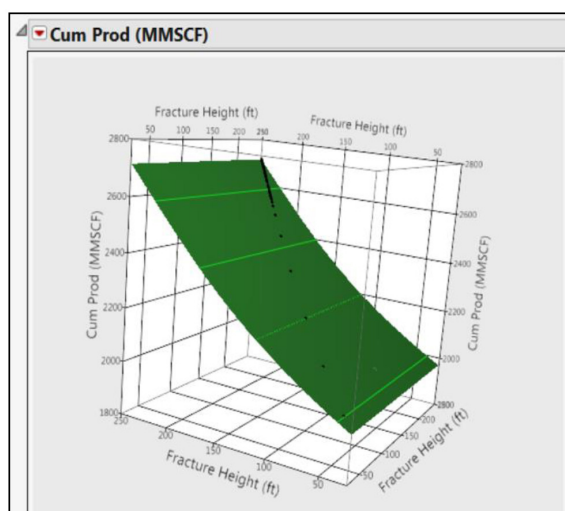


Figure 13—Fracture height vs. cumulative production

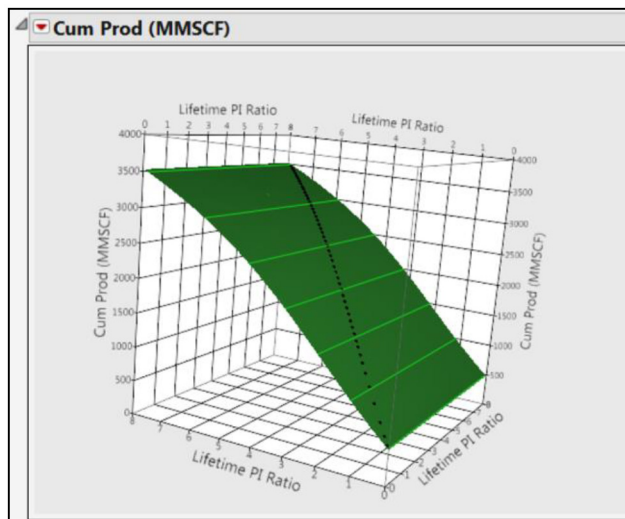


Figure 14—Lifetime PI ratio vs. cumulative production

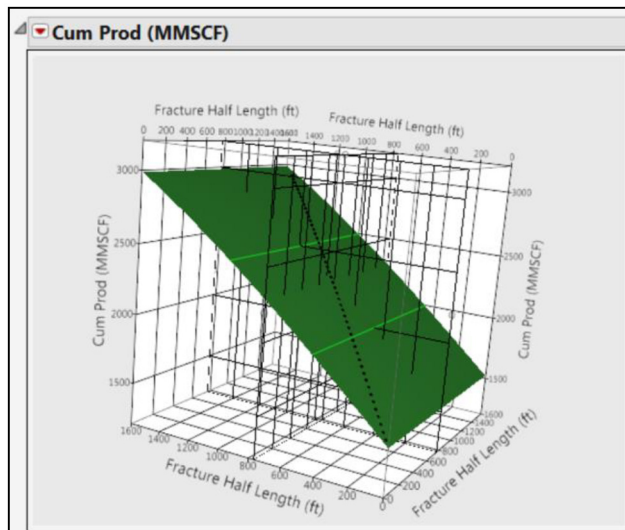


Figure 15—Fracture half-length vs. cumulative production

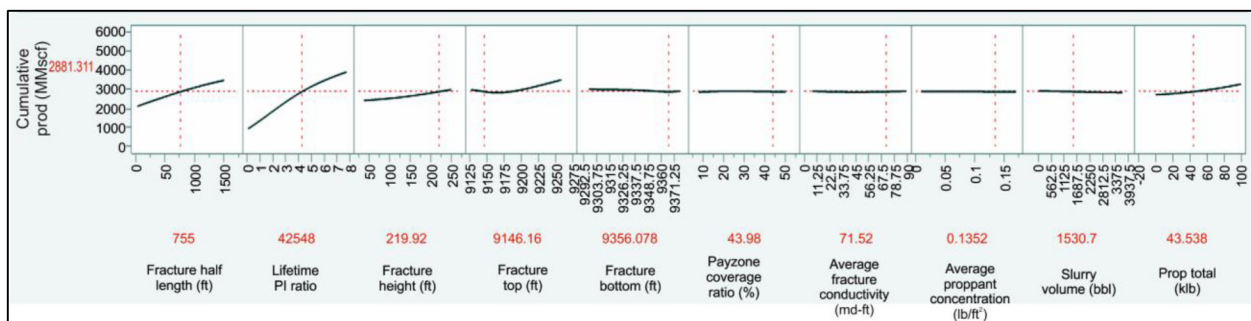


Figure 16—Profiler—inputs vs. output

Data analytics tools have been utilized to analyze the results of a fracture model built with a commercial fracture simulator. Utilization of the fracture simulator with enabled us to investigate the significance of each parameter on the outcome that was used as an input to the data analytics software to analyze the input-output relationship to capture not only the significance of the inputs but also the

direction that the inputs affect the outcome by means of fitting a neural model to the data and displaying it in 3D surface profiler as well as the 2D profiler which were illustrated in figures 8–16. It would not be possible without the use of data analytics tool to clearly show the direction of impact of each input.

The conclusions pertain to this specific model, as neural model that was fit is a data driven model and highly belongs to the model used. However, it serves as a useful illustration as to how the whole workflow is used to investigate the effect of each individual input.

## Acknowledgements

The authors thank Aere Energy (a Shell-ExxonMobil Affiliate), CMGL, and Turkish Petroleum Corp. for their support in publishing this paper.

## References

- Agarwal, R.G., Gardner, D.C., Kleinsteiber, S.W. et al. 1999. Analyzing Well Production Data Using Combined-TypeCurve and Decline-Curve Analysis Concepts. *SPEREE* 478–486.
- Anderson, D. and Mattar, L. 2004. Practical Diagnostics Using Production Data and Flowing Pressures. Presented at the SPE Annual Technical Conference and Exhibition, Houston, Texas, 26–29 September. SPE-89939-MS. <http://dx.doi.org/10.2118/89939-MS>.
- Araya, A. and Ozkan, E. 2002. An Account of Decline-Type-Curve Analysis of Vertical, Fractured, and Horizontal Well Production Data. Presented at the SPE Annual Technical Conference and Exhibition, San Antonio, Texas, 29 September–2 October. SPE-77690-MS. <http://dx.doi.org/10.2118/77690-MS>.
- Arps, J.J. 1945. Analysis of Decline Curves. *Trans of the AIME* **160** (1): 228–247.
- Blasingame, T.A. and Rushing, J.A. 2005. A Production-Based Method for Direct Estimation of Gas in Place and Reserves. Presented at the SPE Eastern Regional Meeting, Morgantown, West Virginia, 14–16 September. SPE-98042-MS. <http://dx.doi.org/10.2118/98042-MS>.
- Bondar, V.V. 2001. *The Analysis of Water-Oil Ratio (WOR) Behavior in Reservoir System*. MS Thesis, Texas A&M University, College Station, Texas (May 2001).
- Butler, R. 1998. SAGD comes of AGE! *J Can Pet Technol* **37** (7): 9–12. PETSOC-98-07-DA. <http://doi.org/10.2118/98-07-DA>.
- Cherian, B.V., Higgins, S.M., Bordakov, G.A. et al. 2014. The Impact of Laminated Rock on Hydraulic Fracture Propagation in Unconventional Resources. Presented at the SPE Energy Resources Conference, Port of Spain, Trinidad and Tobago, 9–11 June. SPE-169960-MS. <http://dx.doi.org/10.2118/169960-MS>.
- Clarkson, C.R. and Pedersen, P.K. 2011. Production Analysis of Western Canadian Unconventional Light Oil Plays. Presented at the Canadian Unconventional Resources Conference, Calgary, Alberta, Canada, 15–17 November. SPE-149005-MS. <http://dx.doi.org/10.2118/149005-MS>.
- Coal Bed Methane Primer New Source of Natural Gas-Environmental Implications Background and Development in the Rocky Mountain West*. 2003. National Energy Technology Laboratory.
- Cramer, D.D. 2008. Stimulating Unconventional Reservoirs: Lessons Learned, Successful Practices, Areas for Improvement. Presented at the SPE Unconventional Reservoirs Conference, Keystone, Colorado, 1–19, February. SPE-114172-MS. <http://doi.org/10.2118/114172-MS>.
- Cramer, D.D., Woo, G.T., and Dawson, J.C. 2004. Development and Implementation of a Low-Polymer-Concentration Crosslinked Fracturing Fluid for Low-Temperature Applications. Presented at the SPE Eastern Regional Meeting, Charleston, West Virginia, 15–17 September. SPE-91418-MS. <http://dx.doi.org/10.2118/91418-MS>.
- Crockett, A.R., Okusu, N.M., and Cleary, M.P. 1986. A Complete Integrated Model for Design and Real-Time Analysis of Hydraulic Fracturing Operations. SPE California Regional Meeting, Oakland, California, 2–4 April. SPE-15069-MS. <http://dx.doi.org/10.2118/15069-MS>.

- Cupcic, F. 2003. The Challenges of Enhanced Recovery. *Extra Heavy Oil and Bitumen: Impact of Technologies on the Recovery Factor* [http://www.google.com/url?sa=t&rct=j&q=cupcicheavyoil&source=web&cd=4&ved=0CC4QFjAD&url=http://www.peakoil.net/iwood2003/ppt/CupcicPresentation.pdf&ei=F8PATqTvD8ikiQK-ismdAw&usg=AFQjCNHOrMjiS5x0nBrC9QWIMF\\_KJDNZNw](http://www.google.com/url?sa=t&rct=j&q=cupcicheavyoil&source=web&cd=4&ved=0CC4QFjAD&url=http://www.peakoil.net/iwood2003/ppt/CupcicPresentation.pdf&ei=F8PATqTvD8ikiQK-ismdAw&usg=AFQjCNHOrMjiS5x0nBrC9QWIMF_KJDNZNw).
- Daneshy, A.A. 1978. Hydraulic Fracture Propagation in Layered Formations. *SPE J.* **18** (1): 33–41. SPE-6088-PA. <http://dx.doi.org/10.2118/6088-PA>.
- Fetkovich, M.J. 1980. Decline Curve Analysis Using Type Curves. *J Pet Technol* **32** (6): 1,065–1,077. SPE-4629-PA. <http://dx.doi.org/10.2118/4629-PA>.
- Fuentes-Cruz, G., Camacho-Velaquez, R., and Vásquez-Cruz, M. 2004. Pressure Transient and Decline Curve Behaviors for Partially Penetrating Wells Completed in Naturally Fractured-Vuggy Reservoirs. Presented at the SPE International Petroleum Conference in Mexico, Puebla, Mexico, 8–9 November. SPE-92116-MS. <http://dx.doi.org/10.2118/92116-MS>.
- Gidley, J.L., Mutti, D.H., Nierode, D.E. et al. 1979. Stimulation of Low-Permeability Gas Formations by Massive Hydraulic Fracturing a Study of Well Performance. *J Pet Technol* **31** (4): 525–531. SPE-6867-PA. <http://dx.doi.org/10.2118/6867-PA>.
- Goktas, B. and Ertekin, T. 1999. A Comparative Analysis of the Production Characteristics of Cavity Completions and Hydraulic Fractures in Coalbed Methane Reservoirs. Presented at the SPE Rocky Mountain Regional Meeting, Gillette, Wyoming, 15–18 May. SPE-55600-MS. <http://dx.doi.org/10.2118/55600-MS>.
- Haskett, W.J. and Brown, P.J. 2005. Recurrent Issues in the Evaluation of Unconventional Resources. *AAPG Studies in Geology* **45** on CD.
- Hou, Z. and Zhou, L. 2011. Modelling and Optimization of Multiple Fracturing Along Horizontal Wellbores in Tight Gas Reservoirs. Presented at the 12th ISRM Congress, Beijing, China, 16–21 October. ISRM-12CONGRESS-2011-238.
- Kabir, C.S. and Izgec, B. 2006. Diagnosis of Reservoir Behavior from Measured Pressure/Rate Data. Presented at the SPE Gas Technology Symposium, Calgary, Alberta, Canada, 15–17 May. SPE-100384-MS. <http://dx.doi.org/10.2118/100384-MS>.
- Li, K. and Horne, R.N. 2005. An Analytical Model for Production Decline-Curve Analysis in Naturally-Fractured Reservoirs. *SPEREE* 197–204.
- Mattar, L. and Anderson, D.M. 2003. A systematic and Comprehensive Methodology for Advanced Analysis of Production Data. Presented at the SPE Technical Conference and Exhibition, Denver, Colorado, 5–8 October. SPE-84472-MS. <http://dx.doi.org/10.2118/84472-MS>.
- Mattar, L., Rushing, J. A., & Anderson, D. M. (2006, January 1). *Production Data Analysis - Challenges, Pitfalls, Diagnostics*. Society of Petroleum Engineers. doi: [10.2118/102048-MS](https://doi.org/10.2118/102048-MS)
- McDaniel, B.W., Grundmann, S.R., Kendrick, W.D. et al. 1997. Field Application of Cryogenic Nitrogen as a Hydraulic Fracturing Fluid. Presented at the SPE Annual Technical Conference and Exhibition, San Antonio, Texas, 5–8 October. SPE-38623-MS. <http://dx.doi.org/10.2118/38623-MS>.
- Meckel, L.D. and Thomasson, M.R. 2008. *Pervasive tight-gas sandstone reservoirs: An overview*.
- Miskimins, J.L. and Barree, R.D. 2003. Modeling of Hydraulic Fracture Height Containment in Laminated Sand and Shale Sequences. Presented at the SPE Production and Operations Symposium, Oklahoma City, Oklahoma, 23–25 March. SPE-80935-MS. <http://dx.doi.org/10.2118/80935-MS>.
- Montgomery, C.T. and Smith, M.B. 2010. Hydraulic Fracturing: History of an Enduring Technology. *J Pet Technol* **62** (12): 26–40. SPE-1210-0026-JPT. <http://dx.doi.org/10.2118/1210-0026-JPT>.

- Rahnema, H., Kharrat, R., and Rostami, B. 2008. Experimental and Numerical Study of Vapor Extraction Process (VAPEX) in Heavy Oil Fractured Reservoir. Presented at the Canadian International Petroleum Conference, Calgary, Alberta, Canada, 17–19 June. PETSOC-2008-116. <http://doi.org/10.2118/2008-116>.
- Reinhardt, B. 2010. Heavy Oil recovery and Usage. *Stanford.edu*, July 3, 2015, from <http://large.stanford.edu/courses/2010/ph240/reinhardt2/>.
- Rieb, B.A. and Leshchyshyn, T.T. 2005. The Production Success of Proppant Stimulation on Horseshoe Canyon Coalbed Methane. Presented at the SPE Annual Technical Conference and Exhibition, Dallas, Texas, 9–12 October. SPE-96864-MS. <http://dx.doi.org/10.2118/96864-MS>.
- Saldungaray, P., Palisch, T., and Shelley, R. 2013. Hydraulic Fracturing Critical Design Parameters in Unconventional Reservoirs. Presented at the SPE Unconventional Gas Conference and Exhibition, Muscat, Oman, 28–30 January. SPE-164043-MS. <http://dx.doi.org/10.2118/164043-MS>.
- Settari, A.T., Bachman, R.C., and Bothwell, P. 2010. Analysis of Nitrogen Stimulation Technique in Shallow CBM Formations. Presented at the SPE Annual Technical Conference and Exhibition, Florence, Italy, 19–22 September. SPE-135683-MS. <http://dx.doi.org/10.2118/135683-MS>.
- Svendson, A.P., Wright, M.S., Clifford, P.J. et al. 1991. Thermally Induced Fracturing of Ula Water Injectors. *SPE Prod Eng* **6** (4): 384–390. SPE-20898-PA. <http://dx.doi.org/10.2118/20898-PA>.
- Vishnukumar, J.N. 2007. Enhanced Coal Bed Methane Recovery Using Nitrogenase Enzyme. Presented at the SPE Annual Technical Conference and Exhibition, Anaheim, California, 11–14 November. SPE-113033-STU. <http://dx.doi.org/10.2118/113033-STU>.
- Warpinski, N.R., Moschovidis, Z.A., Parker, C.D. et al. 1994. Comparison Study of Hydraulic Fracturing Models—Test Case: GRI Staged Field Experiment No. 3 (includes associated paper 28158). *SPE Prod & Fac* **9** (1): 7–16. SPE-25890-PA. <http://dx.doi.org/10.2118/25890-PA>.
- Warpinski, N.R., Clark, J.A., Schmidt, R.A. et al. 1982. Laboratory Investigation of the Effect of In-Situ Stresses on Hydraulic Fracture Containment. *SPE J.* **22** (3): 333–340. SPE-9834-PA. <http://dx.doi.org/10.2118/9834-PA>.
- Williams-Kovacs, J.D. and Clarkson, C.R. 2013. Stochastic Modeling of Multi-Phase Flowback From Multi-Fractured Horizontal Tight Oil Wells. Presented at the SPE Unconventional Resources Conference Canada, Calgary, Alberta, Canada, 5–7 November. SPE-167232-MS. <http://dx.doi.org/10.2118/167232-MS>.
- Zahid, S., Bhatti, A.A., Ahmad Khan, H. et al. 2007. Development of Unconventional Gas Resources: Stimulation Perspective. Presented at the Production and Operations Symposium, Oklahoma City, Oklahoma, 31 March–3 April. SPE-107053-MS. <http://doi.org/10.2523/107053-MS>.

## Appendix

Main Options | Additional Options |

Perform Economic Optimization Based On ...

Fracture Dimensions  
 Treatment Schedule

Fracture Model to Use

3D Shear-Decoupled (Default)  
 3D Tip-Dominated  
 3D Conventional (Linear Elastic)  
 3D Calibrated  
 3D User-Defined  
 2D

Fracpro Model Parameters

Next

Figure A1—Model options

Layers | Rock Properties | Additional Properties | Rock Library | Production Analysis Reservoir Parameters | PVT |

Depth to Middle of Pay	9,280.0 (ft)
Gross Pay Thickness	249.4 (ft)
Net Pay Thickness	249.4 (ft)
Initial Pressure	4,037 (psi)

Permeability	3.084e-03 (mD)
Porosity	0.10 < 1
Water Saturation	0.50 < 1
Young's Modulus	6.997e+06 (psi)

X-Direction Extent	2,500.0 (ft)
<input checked="" type="radio"/> Y-Direction Extent	2,500.0 (ft)
<input type="radio"/> Drainage Area	573.92 (acres)

Fracture Gradient (Closure Stress Gradient)	0.544 (psi/ft)
---	----------------

Wellbore Effects	
Wellbore Hole Diameter (0.0 for no effect)	0.000 (in)
Skin Factor	0.000

Auto

Compaction Effects

Stress Sensitive Reservoir Permeability

Import Reservoir Data

	Effective Vertical Stress (psi)	Permeability Multiplier
1	0	1.0000
2	2,000	1.0000
3	4,000	1.0000
4	6,000	1.0000
5	8,000	1.0000
6	10,000	1.0000
7	12,000	1.0000
8	14,000	1.0000
9	16,000	1.0000
10	18,000	1.0000
11	20,000	1.0000

If you have already run the stimulation model and you are now going to run the reservoir simulator, you can use the button located below.

This button will automatically convert all the information from your reservoir description to a single layer reservoir model with the same properties.

Remember to also import the fracture information on the Fracture Parameters screen.

Import Stimulation Interval Properties

Vertical Stress Gradient

Next

Figure A2—Layer properties

Layers | Rock Properties | Additional Properties | Rock Library | Production Analysis Reservoir Parameters | PVT |

HC Type	Standard Gravity of HC Phase	0.700	Minimum Pressure	15 (psi)
<input checked="" type="radio"/> Gas Well	Reservoir Temperature	250.0 (°F)	Maximum Pressure	4,500 (psi)
<input type="radio"/> Oil Well				
Impurities				
Nitrogen	0.0000 (fraction)	Bubble Point	0 (psi)	
Carbon Dioxide	0.0000 (fraction)	Initial Solution Gas/Oil Ratio	1,250.0 (scf/stb)	
Hydrogen Sulfide	0.0000 (fraction)	Solution Gas Gravity	0.900	

Enter either Bubble Point or SGOR,  
as well as Gas Gravity

Internal PVT Correlation Data

	Pressure (psi)	Formation Volume Factor (rcf/scf)	Viscosity (cp)	Formation Rock Compressibility (1/psi)	Pore Fluid Compressibility (1/psi)
1	15	1.36E+00	0.012	4.8623E-06	6.8027E-02
2	239	8.25E-02	0.013	4.8623E-06	4.1847E-03
3	463	4.19E-02	0.013	4.8623E-06	2.1588E-03
4	687	2.78E-02	0.014	4.8623E-06	1.4546E-03
5	912	2.07E-02	0.014	4.8623E-06	1.0968E-03
6	1,136	1.64E-02	0.014	4.8623E-06	8.8026E-04
7	1,360	1.36E-02	0.015	4.8623E-06	7.3514E-04
8	1,585	1.16E-02	0.015	4.8623E-06	6.3109E-04
9	1,809	1.01E-02	0.016	4.8623E-06	5.5285E-04
10	2,033	8.97E-03	0.016	4.8623E-06	4.9188E-04
11	2,257	8.07E-03	0.017	4.8623E-06	4.4300E-04
12	2,482	7.36E-03	0.017	4.8623E-06	4.0296E-04
13	2,706	6.77E-03	0.018	4.8623E-06	3.6957E-04
14	2,930	6.29E-03	0.018	4.8623E-06	3.4128E-04
15	3,154	5.88E-03	0.019	4.8623E-06	3.1702E-04
16	3,379	5.54E-03	0.019	4.8623E-06	2.9597E-04
17	3,603	5.25E-03	0.020	4.8623E-06	2.7755E-04
18	3,827	4.99E-03	0.020	4.8623E-06	2.6129E-04

Next

Figure A3—PVT properties

Layers | Rock Properties | Additional Properties | Rock Library | Production Analysis Reservoir Parameters | PVT |

	Name
1	Sandstone
2	Limestone
3	Granite
4	Shale
5	Dolomite
6	Soft Coal
7	Hard Coal
8	User Spec 1
9	User Spec 2
10	User Spec 3
11	User Spec 4
12	User Spec 5
13	User Spec 6
14	User Spec 7
15	User Spec 8

Add New Rock Type to List  
Remove Rock Type from List  
Create User Defined Rock Type  
Edit/View Rock Type Info  
  
Save Rocktype to User Library  
Delete Rocktype from User Library

Next

Figure A4—Rock library

Layers | Rock Properties | Additional Properties | Rock Library | Production Analysis Reservoir Parameters | PVT |

Reservoir Type     Single Layer     Multi Layer     HC Type     Gas Well     Oil Well

Leakoff Fluid Permeability Ratio Kp/Kl	10.00
Reservoir Pore Pressure	4,037 (psi)
Average Pressure in Fracture for Leakoff Coeff. <-> Perm Calc	5,550 (psi)
Total Compressibility (Ct)	2.48e-04 (1/psi)
Pore Fluid Viscosity	0.030 (cp)
Porosity	0.100
Water Saturation	0.00
Gas-in-Foam Leakoff Percentage	100.00 (%)

Set to Gas Defaults     Set to Oil Defaults     Drainage Area     Reservoir Depletion     Not Used

X-Direction Extent	2,500.0 (ft)
Y-Direction Extent	2,500.0 (ft)
Well Spacing	573.9 (acres)

Fracture Azimuth    0.0 (deg)    Suggest Compressibility and Viscosity     Ct Calculator    Pore Fluid Compressibility    2.48e-04 (1/psi)    Rock Compressibility    2.16e-07 (1/psi)    Calculate Ct   

Figure A5—Additional properties

Layers | Rock Properties | Additional Properties | Rock Library | Production Analysis Reservoir Parameters | PVT |

Mechanical Properties     Chemical Properties     Thermal Properties

Rock-Type	Calcite Fraction (% mass)	Dolomite Fraction (% mass)	Ref. Temp (°F)	Rxn Rate Constant (see #1 below)	Reaction Order	Activation Energy (kcal/mol)	Rock Embedment Strength (psi)	Specific Gravity	Specific Heat (Btu/lb °F)	Thermal Cond (Btu/ft hr °F)
1 Sandstone	0.00	0.00	150.0	0.00E+00	0.000	0.00	80,000	2.65	0.26	2.57
2 Limestone	100.00	0.00	150.0	7.30E-04	0.410	6.03	40,000	2.72	0.21	0.91
3 Granite	0.00	0.00	150.0	0.00E+00	0.000	0.00	100,000	2.70	0.20	1.74
4 Shale	0.00	0.00	150.0	0.00E+00	0.000	0.00	80,000	2.60	0.20	1.01
5 Dolomite	0.00	100.00	150.0	1.43E-04	0.500	8.50	80,000	2.86	0.21	0.91
6 Soft Coal	0.00	0.00	150.0	0.00E+00	0.000	0.00	80,000	1.30	0.20	0.91
7 Hard Coal	0.00	0.00	150.0	0.00E+00	0.000	0.00	80,000	1.30	0.20	0.91
8 User Spec 1	100.00	0.00	150.0	0.00E+00	0.000	0.00	80,000	2.60	0.20	1.70
9 User Spec 2	0.00	0.00	150.0	0.00E+00	0.000	0.00	80,000	2.60	0.20	1.70
10 User Spec 3	0.00	0.00	150.0	0.00E+00	0.000	0.00	80,000	2.60	0.20	1.70
11 User Spec 4	0.00	0.00	150.0	0.00E+00	0.000	0.00	80,000	2.60	0.20	1.70
12 User Spec 5	0.00	0.00	150.0	0.00E+00	0.000	0.00	80,000	2.60	0.20	1.70
13 User Spec 6	0.00	0.00	150.0	0.00E+00	0.000	0.00	80,000	2.60	0.20	1.70
14 User Spec 7	0.00	0.00	150.0	0.00E+00	0.000	0.00	80,000	2.60	0.20	1.70
15 User Spec 8	0.00	0.00	150.0	0.00E+00	0.000	0.00	80,000	2.60	0.20	1.70

#1 - ((mol/cm<sup>3</sup>)<sup>m</sup>(1-m) cm/sec) where m is the reaction order.

Figure A6—Rock properties

Layers   Rock Properties   Additional Properties   Rock Library   Production Analysis Reservoir Parameters   PVT					
Reservoir Data-Entry Options					
<input checked="" type="radio"/> Lithology-Based	<input checked="" type="radio"/> General Multi-Scale	<input type="radio"/> General Single Scale			
Depth TVD (ft)	Layer Thickness (in)	Rock Type	Depth TVD (ft)	Stress (psi)	
1 0.0	9,020.0	Sandstone	1 0.0	8,100	
2 9,020.0	500.0	Sandstone	2 9,030.0	7,400	
3 9,520.0	0.0	Sandstone	3 9,070.0	7,900	
4 0.0	0.0		4 9,115.0	7,250	
5 0.0	0.0		5 9,155.0	6,900	
6 0.0	0.0		6 9,170.0	6,050	
7 0.0	0.0		7 9,200.0	5,500	
8 0.0	0.0		8 9,250.0	5,050	
9 0.0	0.0		9 9,310.0	5,750	
10 0.0	0.0		10 9,340.0	6,550	
11 0.0	0.0		11 9,360.0	7,500	
12 0.0	0.0		12 9,380.0	6,700	
13 0.0	0.0		13 9,435.0	6,800	
14 0.0	0.0		14 9,455.0	8,050	
15 0.0	0.0		15 9,475.0	8,500	
16 0.0	0.0		16 9,575.0	7,950	
17 0.0	0.0		17 0.0	0	
18 0.0	0.0		18 0.0	0	
19 0.0	0.0		19 0.0	0	
20 0.0	0.0		20 0.0	0	
21 0.0	0.0		21 0.0	0	
22 0.0	0.0		22 0.0	0	

Depth Entry Mode  Enter TVD  Enter Permeability  Enter Leakoff Coefficient

Fluid Loss Entry Mode  Enter Permeability  Enter Leakoff Coefficient

Set Composite Layering Effect from  Table Entry  Payzone Flag Composite Layering Effect  Outside Payzone 1.00

Perforations Depth to Top of Perfs 9,225 (ft) Depth to Bot of Perfs 9,330 (ft) Initial Frac Depth 9,280 (ft)

Reservoir Temperature 240 (°F) Logs/Layers Editor Layer Display Next

Figure A7—layers

Fluid Selection   Proppant Selection			
Fluid Selection Criteria		Library and Vendor Selection	
Reservoir Temperature 240 (°F)			Fluid Library Selection
Minimum App. Viscosity 200.0 (cp) @ 40 (1/sec) after 1.0 (hr)			All
Average Permeability 3.084e-03 (mD)			Vendor Selection
Reservoir Pressure 4,037 (psi)			All
<input type="checkbox"/> Reservoir is Water-Sensitive			<input type="button" value="Edit Current Fluid"/>
<input type="checkbox"/> Reservoir Produces Dry Gas			
<input type="checkbox"/> Reservoir Requires KCl for Clay Control			
Qualifying Fluids			
Fluid System	Vendor	Min Gel Loading (lb/Mgal)	App. Viscosity (cp)
1 Hybor	Halliburton	50.00	887.54
2 Emerald FRAQ D	Baker	25.00	642.69
3 Spectra Frac	BJ Services	25.00	617.65
4 Spectra Frac DF	BJ Services	25.00	578.20
5 Viking	BJ Services	30.00	573.33
<input type="button" value="Move Up"/>		<input type="button" value="Move Down"/>	<input type="button" value="Add"/>
<input type="button" value="Remove"/>		<input type="button" value="Add Fluid from Library"/>	
<input type="button" value="Add Proprietary Fluid from Library"/>			
Selected Fluids		1 2% KCl 2% KCl 0.00 0.96 0.00	
Results Plots			
<input type="button" value="App. Visc vs Time"/>		<input type="button" value="Friction Pressure vs Rate"/>	
			<input type="button" value="Next"/>

Figure A8—Fluid selection

Fluid Selection Proppant Selection

Proppant Selection Criteria	6.774 (psi)	Library and Type Selection						
Closure Stress	1.000 (psi)	Proppant Library Selection All						
Bottomhole Flowing Pressure	5.774 (psi)	Proppant Type Selection All						
Effective Stress on Proppant	3.084e-03 (mD)	<= Size <=						
Average Payzone Permeability								
Proppant Damage	0.50							
Proppant Damage Factor								
Non-Darcy and Multi-Phase Effects Not Used		Proppant Perm Damage						
Edit Selected Proppant								
Qualifying Proppants								
Proppant System	Vendor	Mesh Size	Apparent Damage Factor	Total Damage Factor	Cond for 2 PSF (mD ft)	Proppant Cost (\$/lb)	Cond Cost (\$/mD ft)	
1 Sand	Other	100/100	0.00	0.50	50.20	0.00	0.00E+00	
2 Accupak	Urimin	20/40	0.00	0.50	969.07	0.00	0.00E+00	
3 AcPack	Borden	20/40	0.00	0.50	3.20E 58	0.00	0.00E+00	
4 Arizona Sand	Other	12/20	0.00	0.50	2,970.00	0.00	0.00E+00	
5 Arizona Sand	Other	16/30	0.00	0.50	2,296.25	0.00	0.00E+00	

Move Up | Move Down | Add | Remove | Add Proppant from Library

Selected Proppants

1 Brady Sand	GENERIC	20/40	0.00	0.50	618.89	0.07	2.26E-04
--------------	---------	-------	------	------	--------	------	----------

Next

Figure A9—Proppant selection

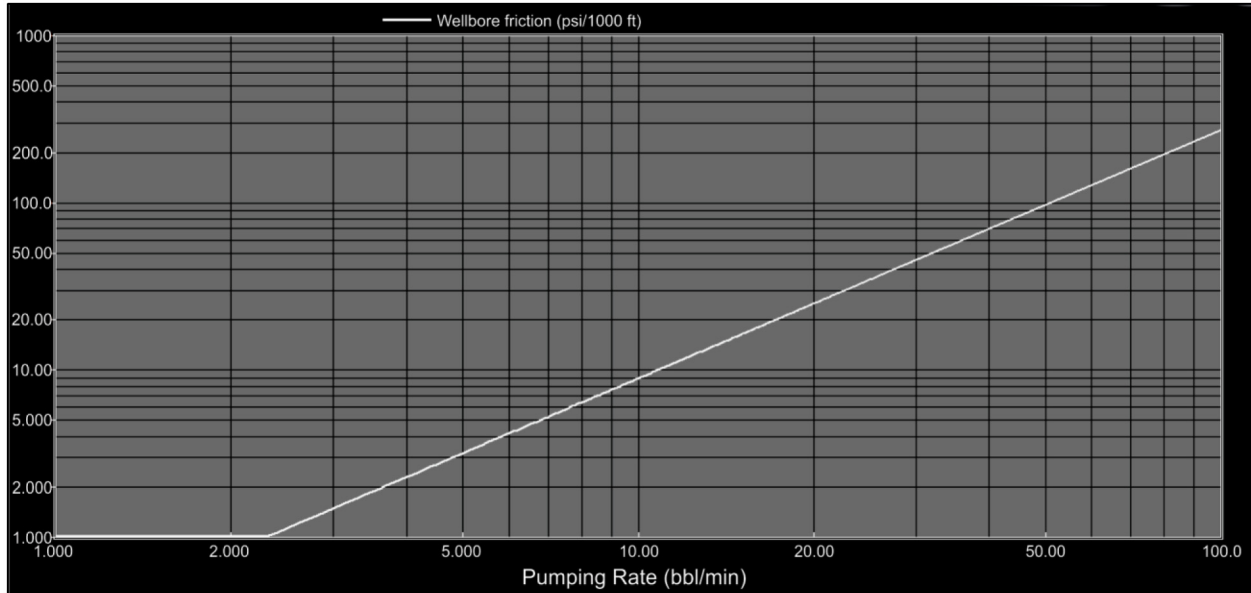


Figure A10—Wellbore friction vs. pumping rate

Production Constraints		Filtrate Cleanup Effects		
Time Step (#)	Time Interval (days)	Total Time (days)	Maximum HC Rate (Mscf/d)	Minimum Pressure (psi)
1	0.250	0.25	6,000.0	3,000 Bottomhole
2	0.250	0.50	6,000.0	3,000 Bottomhole
3	0.500	1.00	6,000.0	3,000 Bottomhole
4	1.000	2.00	6,000.0	2,000 Bottomhole
5	28.000	30.00	6,000.0	2,000 Bottomhole
6	152.500	182.50	6,000.0	2,000 Bottomhole
7	182.500	365.00	6,000.0	2,000 Bottomhole
8	730.000	1095.00	6,000.0	1,000 Bottomhole
9	1,095.000	2190.00	6,000.0	1,000 Bottomhole
10	1,460.000	3650.00	6,000.0	1,000 Bottomhole
11	0.000		0.0	0
12	0.000		0.0	0
13	0.000		0.0	0
14	0.000		0.0	0
15	0.000		0.0	0
16	0.000		0.0	0
17	0.000		0.0	0
18	0.000		0.0	0
19	0.000		0.0	0
20	0.000		0.0	0
21	0.000		0.0	0
22	0.000		0.0	0

Minimum HC Rate  Maximum Drawdown

Set Up Table for Designed Production Constraints

Total Production Time <input type="text" value="3,650.0 (days)"/>	Pressure Location <input type="button" value="Bottomhole"/>
Maximum HC Rate <input type="text" value="6,000.0 (Mscf/d)"/>	
Minimum Pressure <input type="text" value="3,000 (psi)"/>	<input type="button" value="Set Up Table"/>

Figure A11—Production constraints

Production Constraints		Filtrate Cleanup Effects	
Total Volume of Filtrate Pumped	<input type="text" value="10,000.0 (bbls)"/>		
Filtrate Viscosity	<input type="text" value="3.00 (cp)"/>		
Invaded Region Damage Factor	<input type="text" value="75.00 (%)"/>		
Number of Pore Volumes Produced to Achieve 50% Filtrate Cleanup	<input type="text" value="10.0"/>		

Figure A12—Filtrate cleanup effects

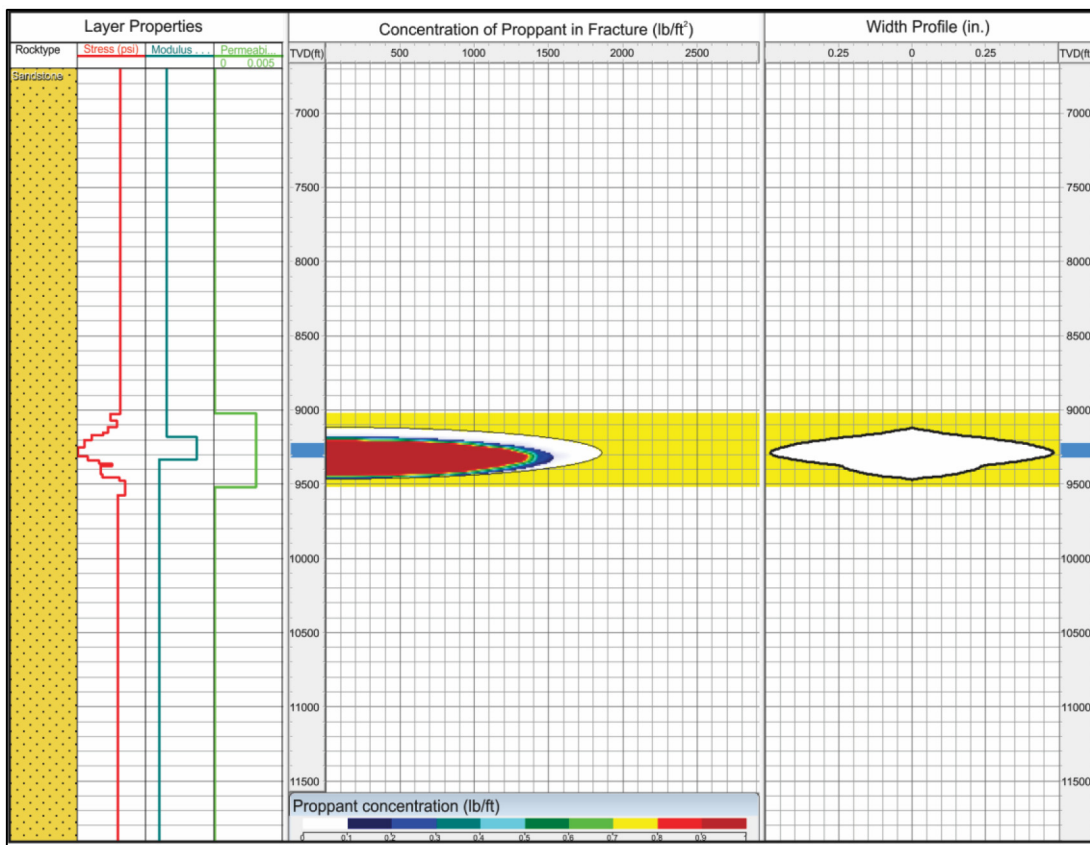


Figure A13—Concentration of proppant in fracture

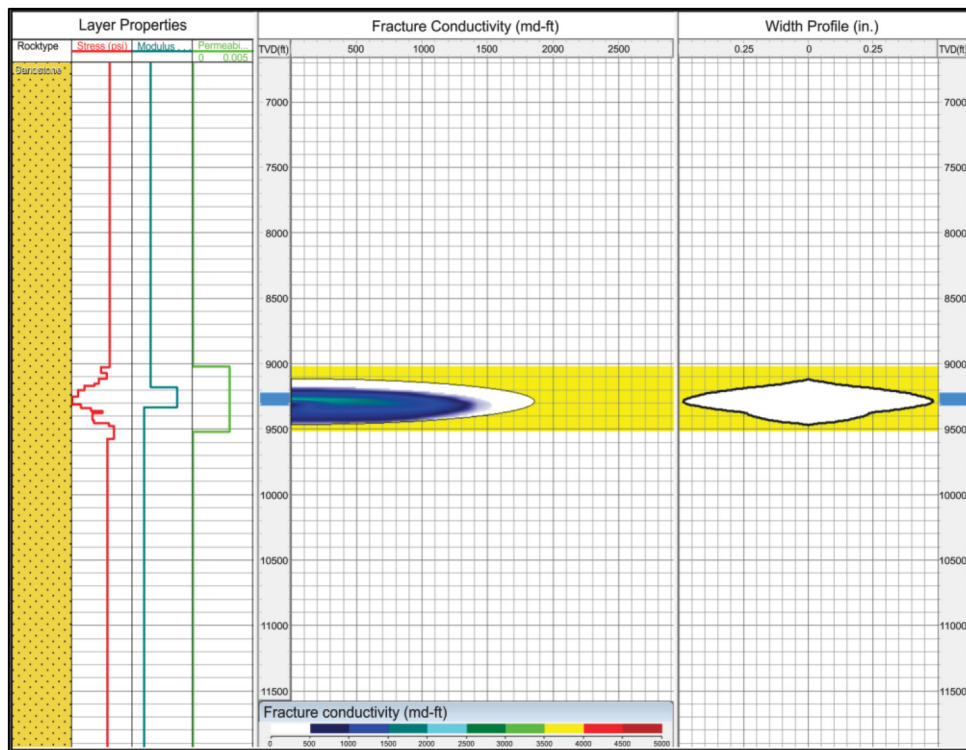


Figure A14—Fracture conductivity

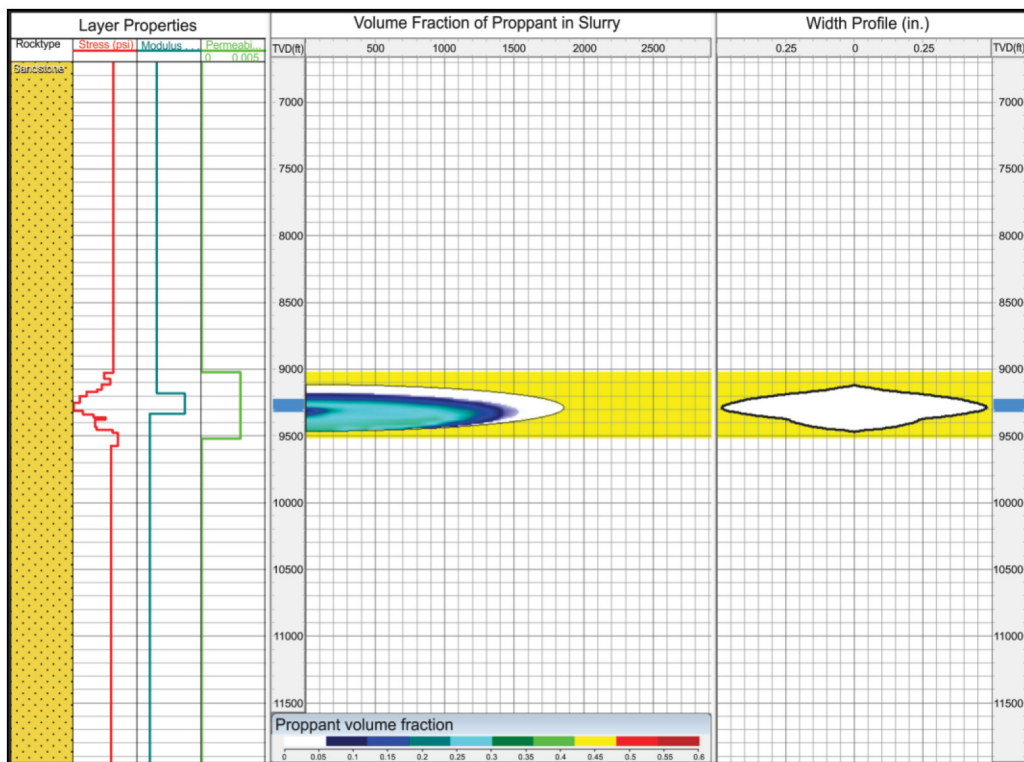


Figure A15—Proppant volume fraction profile

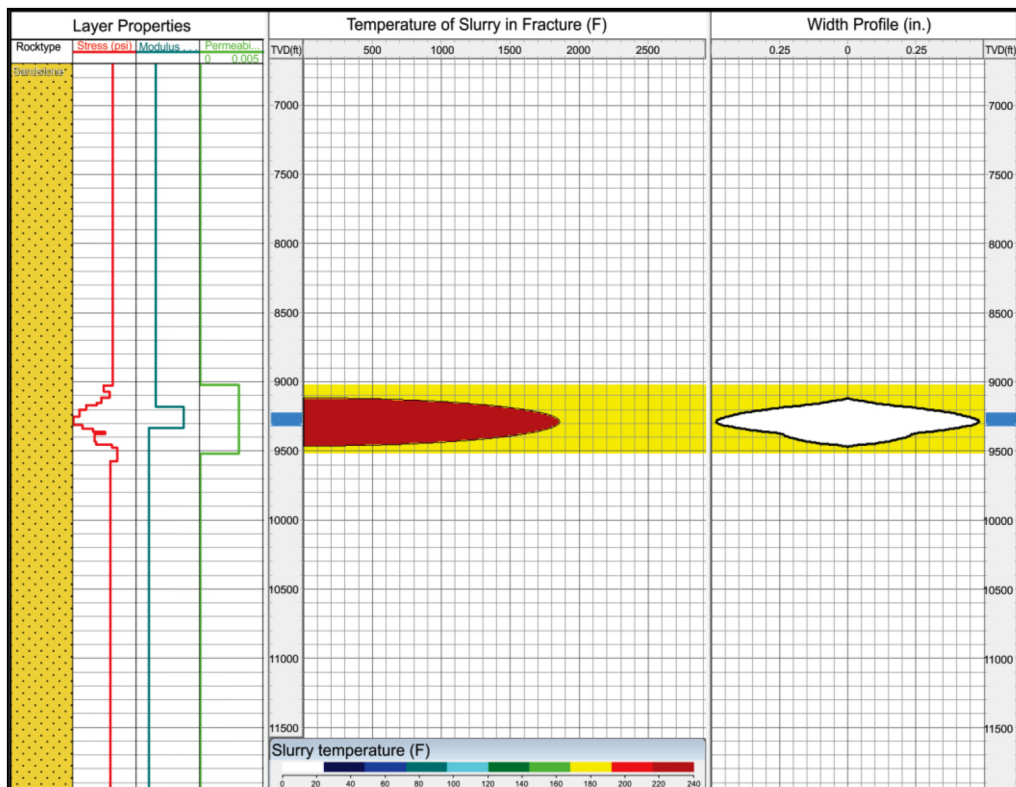


Figure A16—Slurry temperature profile

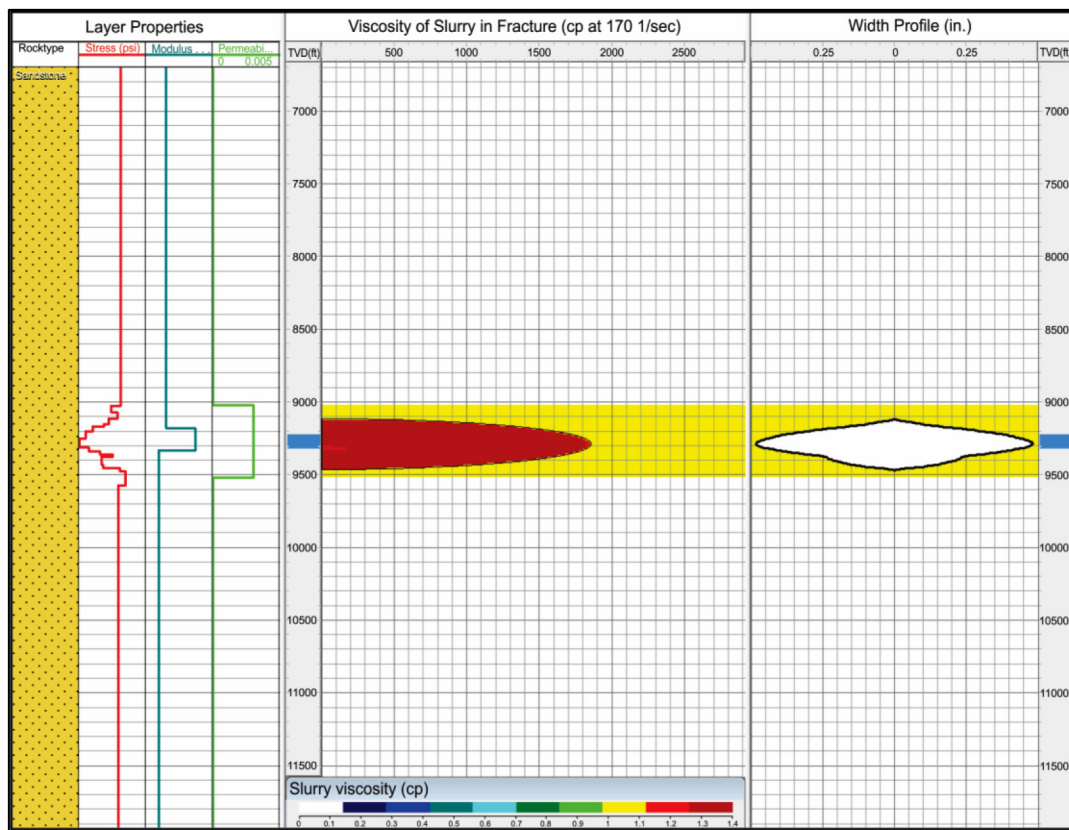


Figure A17—Slurry viscosity profile

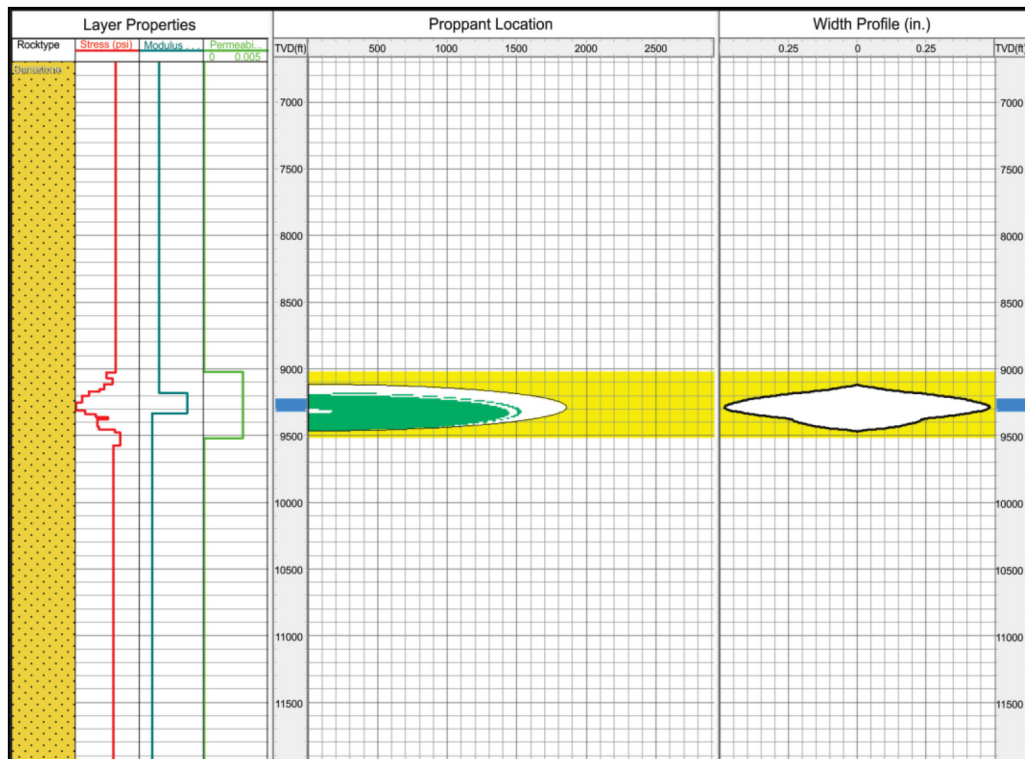


Figure A18—Proppant location profile

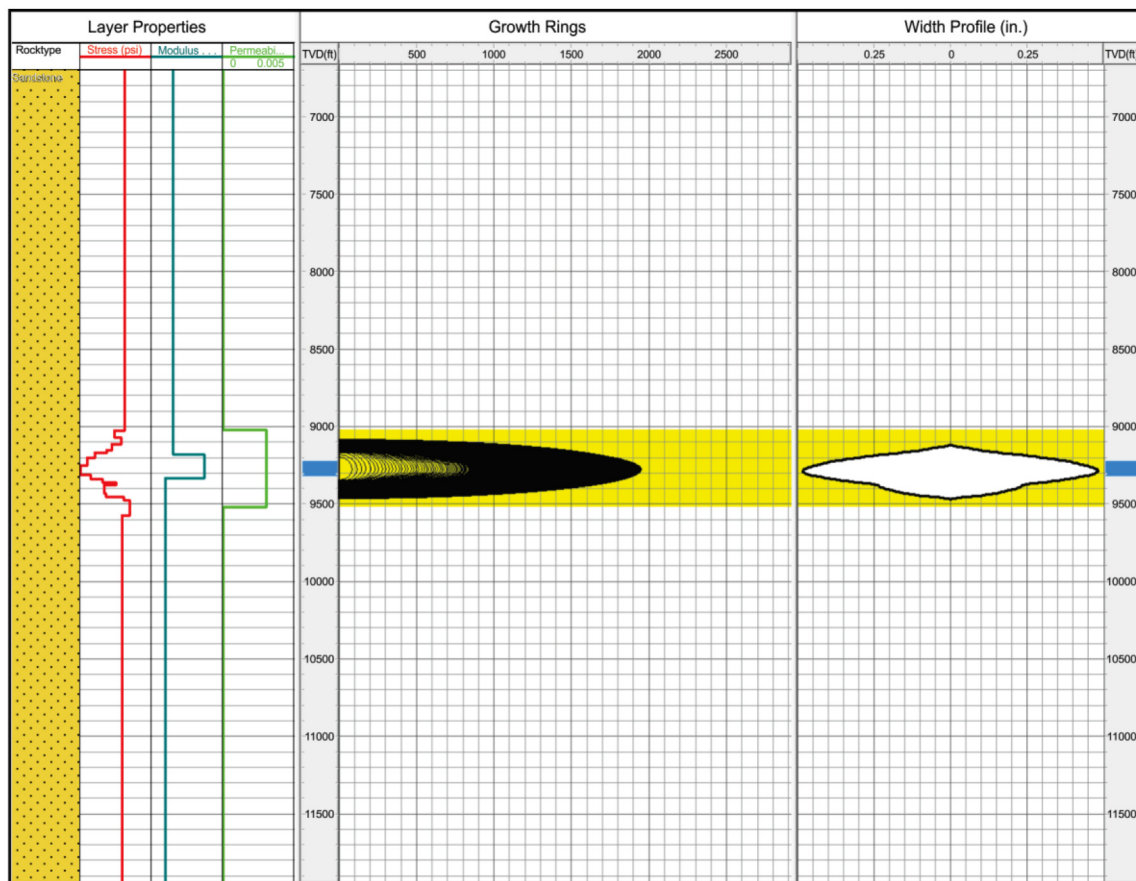


Figure A19—Growth rings

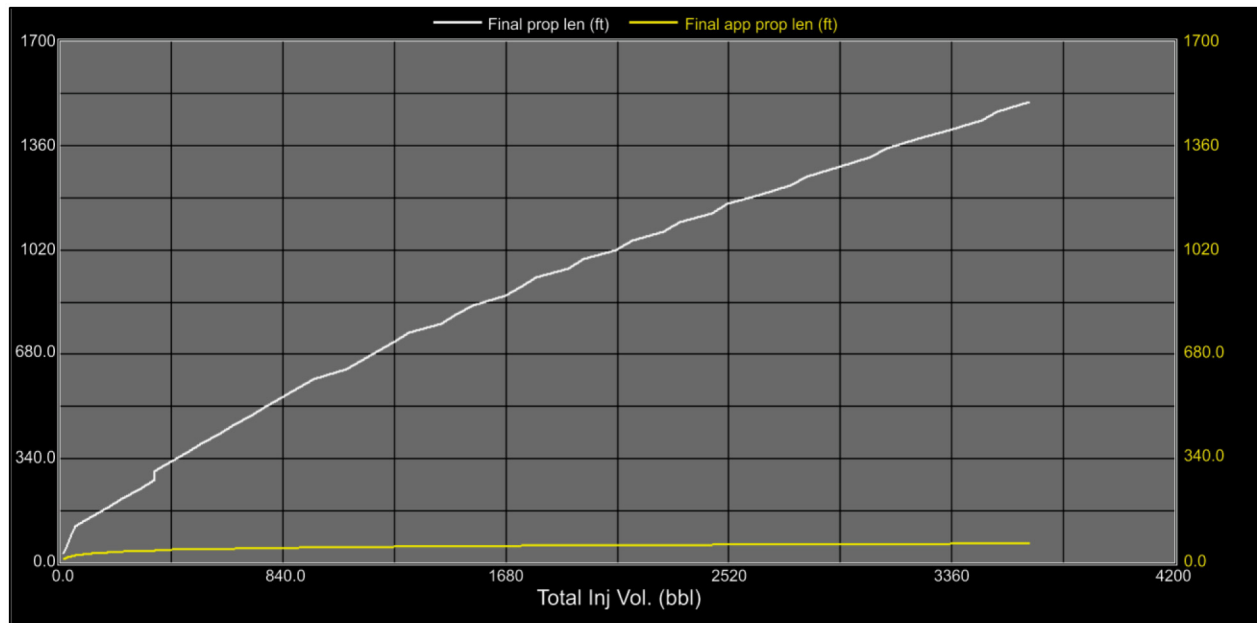


Figure A20—Final prop. length vs. total inj. volume

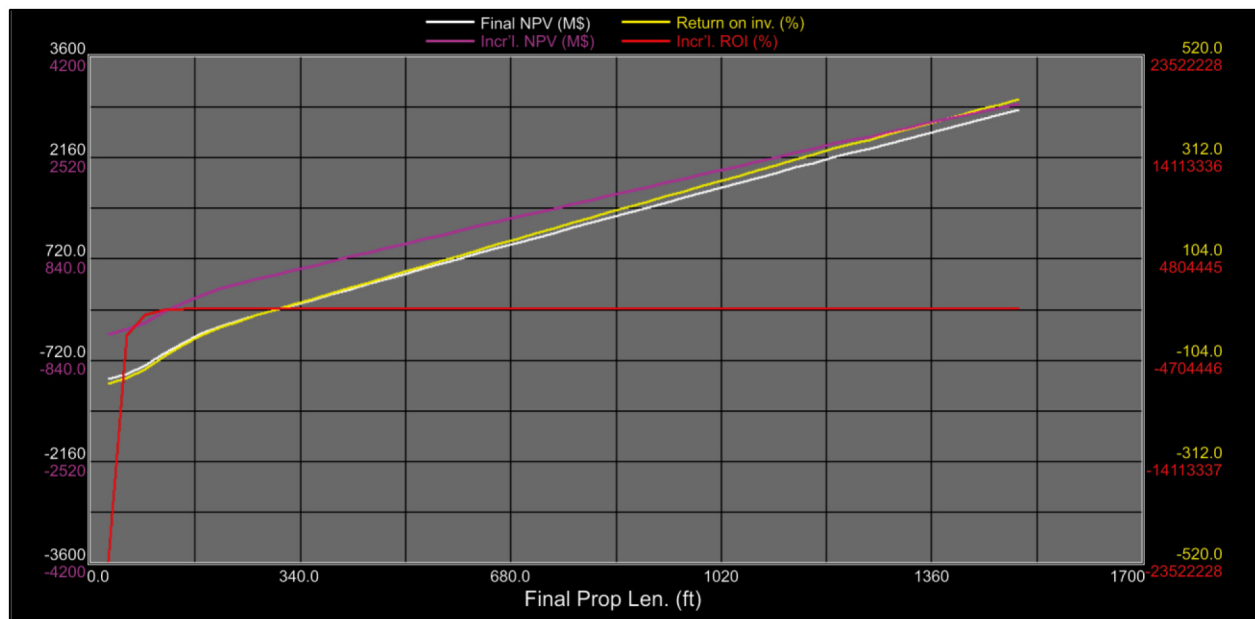


Figure A21—NPV vs. final pro. length

A robust commercial statistical tool has been used to analyze the relationship between the inputs and output.

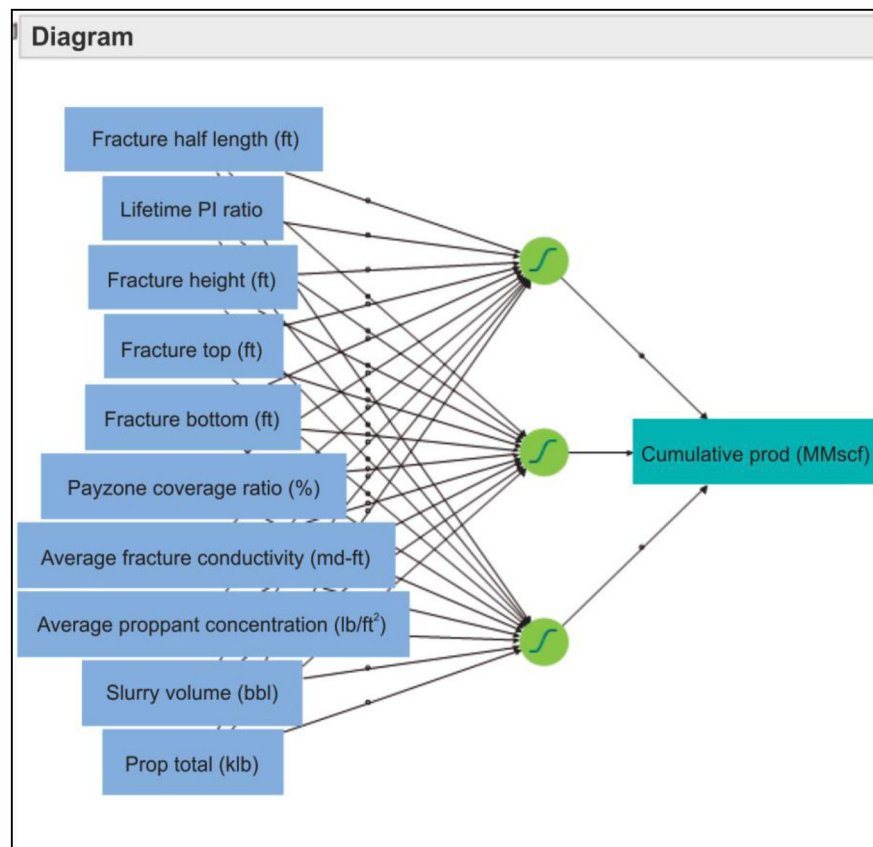


Figure A22—Input-output diagram

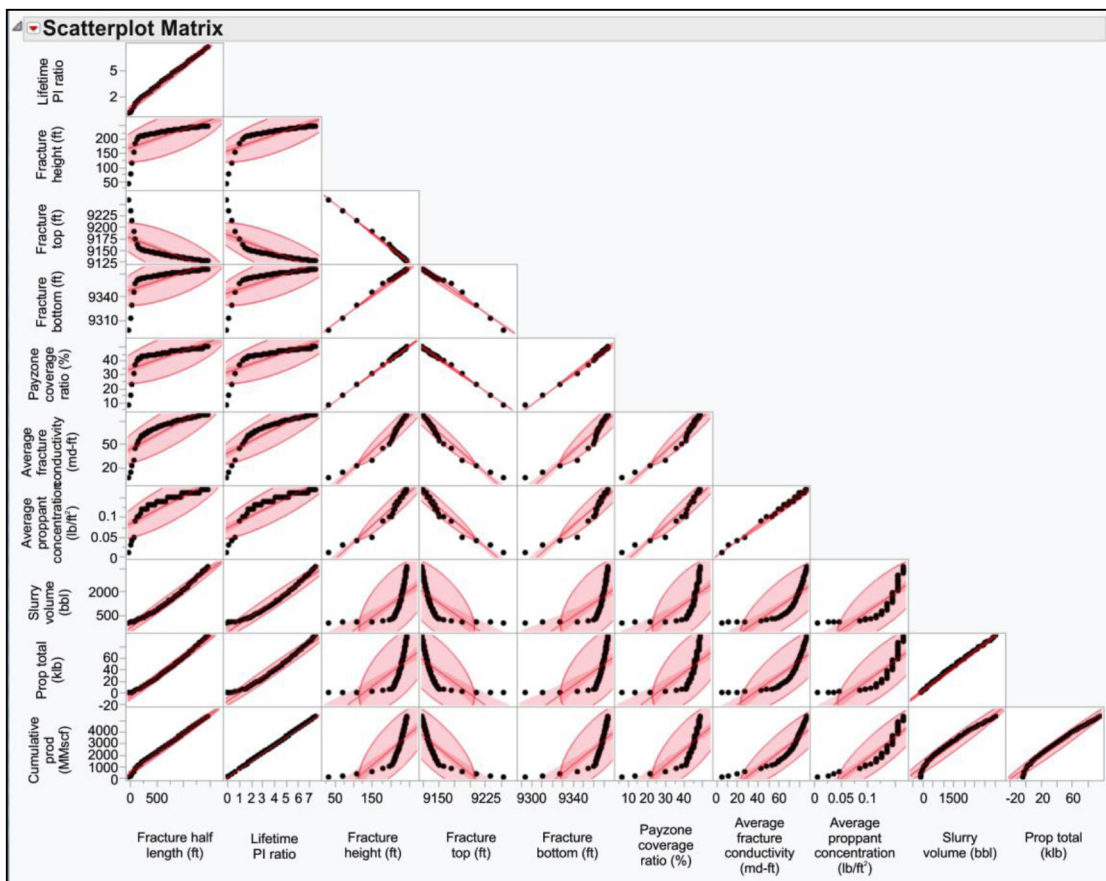


Figure A23—Scatterplot matrix

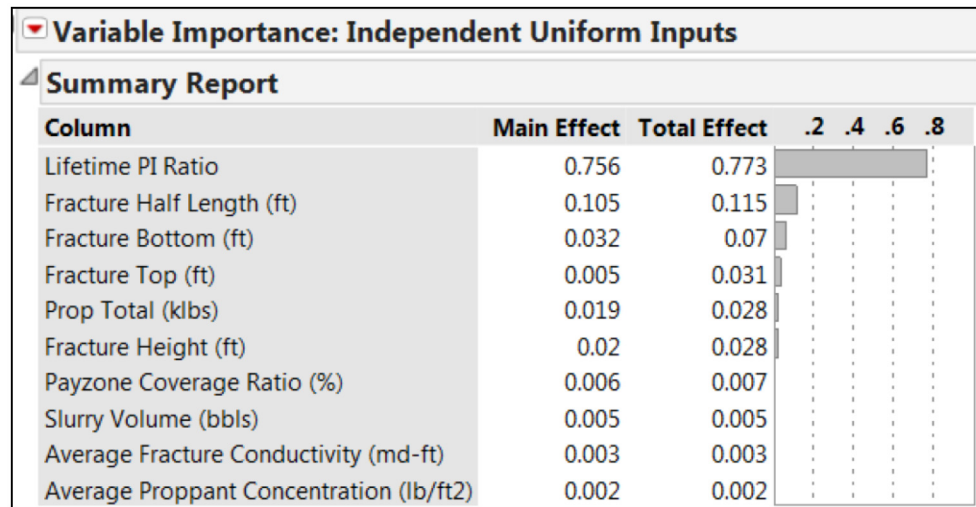


Figure A24—Variable importance